



1 **Organic carbon at a remote site of the western**  
2 **Mediterranean Basin: composition, sources and chemistry**  
3 **during the ChArMEx SOP2 field experiment**

4 Vincent Michoud<sup>1,2,3</sup>, Jean Sciare<sup>4,5</sup>, Stéphane Sauvage<sup>1,2</sup>, Sébastien Dusanter<sup>1,2,6</sup>, Thierry  
5 Léonardis<sup>1,2</sup>, Valérie Gros<sup>4</sup>, Cerise Kalogridis<sup>4</sup>, Nora Zannoni<sup>4</sup>, Anaïs Féron<sup>4</sup>, Jean-Eudes  
6 Petit<sup>4,7,\*</sup>, Vincent Crenn<sup>4</sup>, Dominique Baisnée<sup>4</sup>, Roland Sarda-Estève<sup>4</sup>, Nicolas Bonnaire<sup>4</sup>,  
7 Nicolas Marchand<sup>8</sup>, H. Langley DeWitt<sup>8</sup>, Jorge Pey<sup>8,\*\*</sup>, Aurélie Colomb<sup>9</sup>, François Gheusi<sup>10</sup>,  
8 Sonke Szidat<sup>11</sup>, Iasonas Stavroulas<sup>5</sup>, Agnès Borbon<sup>3,\*\*\*</sup>, Nadine Locoge<sup>1,2</sup>

9

10 [1] Mines Douai, SAGE, F-59508, Douai, France

11 [2] Université de Lille, 59655, Villeneuve d'Ascq, France

12 [3] LISA, UMR-CNRS 7583, Université Paris Est Créteil (UPEC), Université Paris Diderot (UPD), Institut  
13 Pierre Simon Laplace (IPSL), Créteil, France

14 [4] LSCE, IPSL, CEA et Université de Versailles, CNRS, Saint-Quentin, France

15 [5] The Cyprus Institute, Energy Environment Water Research Center, Nicosia, Cyprus

16 [6] School of Public and Environmental Affairs, Indiana University, Bloomington, IN, USA

17 [7] INERIS, 60550 Verneuil-en-Halatte, France

18 [8] Aix Marseille Univ, CNRS, LCE, Marseille, France

19 [9] LaMP, UMR-CNRS 6016, Clermont Université, Université Blaise Pascal, Aubière, France

20 [10] Laboratoire d'Aérodynamique, Université de Toulouse, CNRS, Toulouse, France

21 [11] Department of Chemistry and Biochemistry & Oeschger Centre for Climate Change Research,  
22 University of Bern, Bern, Switzerland

23

24 \*now at Air Lorraine, 20 rue Pierre Simon de Laplace, 57070 Metz, France

25 \*\*now at the Geological Survey of Spain, 50006 Zaragoza (Spain)

26 \*\*\*now at LaMP, UMR-CNRS 6016, Clermont Université, Université Blaise Pascal, Aubière, France

27

28 Corresponding authors :

29 V. Michoud ([vincent.michoud@lisa.u-pec.fr](mailto:vincent.michoud@lisa.u-pec.fr))

30 S. Sauvage ([stephane.sauvage@mines-douai.fr](mailto:stephane.sauvage@mines-douai.fr))

31

32 **Abstract**

33



1           The ChArMEx (Chemistry and Aerosol Mediterranean Experiment) SOP2 (Special  
2 Observation Period 2) field campaign took place from 15 July to 05 August 2013 in the  
3 western Mediterranean basin, at Ersa a remote site in Cape Corsica. During the campaign  
4 more than 80 Volatile Organic Compounds (VOCs), including oxygenated species were  
5 measured by different online and offline techniques. At the same time an exhaustive  
6 description of the chemical composition of fine aerosols was performed. First we combined a  
7 back-trajectory analysis and an estimation of photochemical age to characterize air mass  
8 origins and chemical processing times, which confirmed the remote nature of the site.  
9 Therefore, low levels of anthropogenic VOCs (typically tens to hundreds of ppt for individual  
10 species) and black carbon ( $0.1\text{--}0.9 \mu\text{g m}^{-3}$ ) were observed while significant levels of biogenic  
11 species (peaking at ppb level) were measured. Furthermore, secondary oxygenated VOCs  
12 (OVOCs) largely dominated the VOC speciation during the campaign, while Organic Matter  
13 (OM) dominated the aerosol chemical composition (55% of the total mass of non-refractory  
14 submicron aerosol on average).

15           Second, Positive Matrix Factorization (PMF) and Concentration Field (CF) analyses  
16 were performed on a database containing 42 VOCs (or grouped VOCs), including OVOCs, to  
17 identify co-variation factors of compounds that are representative of primary emissions, or  
18 chemical transformation processes. A six-factor solution was found for the PMF analysis,  
19 including a primary and secondary biogenic factor, both correlated to temperature and  
20 exhibiting a clear diurnal profile. In addition, three anthropogenic factors characterized by  
21 compounds of various lifetimes and/or sources have been identified (long-lived, medium-  
22 lived and short-lived anthropogenic factors). The anthropogenic nature of these factors was  
23 confirmed by the CF analysis which identified potential source areas known for intense  
24 anthropogenic emissions (north of Italy and south-east of France). Finally, a factor  
25 characterized by OVOCs of both biogenic and anthropogenic origins was found. This factor  
26 was well correlated to submicron organic aerosols (OA) measured by an Aerosol Chemical  
27 Speciation Monitor (ACSM) highlighting the close link between OVOCs and organic aerosols  
28 measured at Cape Corsica mainly associated (96%) to secondary fraction of OA. The source  
29 apportionment of OA measured by ACSM led to a 3-factor solution identified as Hydrogen-  
30 like OA (HOA), Semi-Volatile-Oxygenated OA (SV-OOA) and Low-Volatile OOA (LV-  
31 OOA) for averaged mass concentration of  $0.13$ ,  $1.59$ , and  $1.92 \mu\text{g m}^{-3}$ , respectively.

32           A combined analysis of gaseous PMF factors with inorganic and organic fractions of  
33 aerosols helped distinguishing between anthropogenic/continental and biogenic influences on  
34 the aerosol and gas phase compositions.



1

2 **1 Introduction**

3

4       Organic matter is directly emitted in the atmosphere both in the gas phase as Volatile  
5 Organic Compounds (VOCs) and in the aerosol phase as Primary Organic Aerosol (POA).  
6 The sources can be of biogenic (from land or marine ecosystems) and anthropogenic (from  
7 traffic, industrial activities or residential heating) origins. Once emitted, it can be transported  
8 over long distances and undergo chemical transformations due to atmospheric photo-oxidants  
9 such as ozone (O<sub>3</sub>), the hydroxyl radical (OH) and the nitrate radical (NO<sub>3</sub>) at night. The  
10 hydroxyl radical is the main oxidant in the atmosphere and, therefore, controls the fate of  
11 most VOCs through oxidation cycles that lead to the formation of tropospheric O<sub>3</sub> (Seinfeld  
12 and Pandis, 1998) and of a large number of secondary Oxygenated VOCs (OVOCs)  
13 (Atkinson et al., 2000, Goldstein and Galbally, 2007). OVOCs subsequently react with  
14 atmospheric oxidants leading to multi-functionalized compounds of lower volatility through a  
15 multigenerational oxidation process (Kroll and Seinfeld, 2008; Jimenez et al., 2009, Aumont  
16 et al., 2012). These semi-volatile compounds take part in the formation of Secondary Organic  
17 Aerosols (SOA) by condensation onto pre-existing particles (Kanakidou et al., 2005). Organic  
18 aerosols are of particular interest owing to their impact on human health (Pope and Dockery,  
19 2006) and their direct (Forster et al., 2007) or indirect (Lohmann and Feichter, 2005) effect on  
20 earth's climate. Furthermore, chemical models suggest that the secondary organic gaseous  
21 fraction, still reactive and multi-functionalized several days after emission, can be transported  
22 over long distances, affecting the oxidant budget as well as the formation of ozone and SOA,  
23 at remote locations (Aumont et al., 2005; Madronich, 2006). It is therefore essential to  
24 understand the sources and fate of organic matter in the atmosphere, and especially its  
25 evolution during long range transport.

26       Positive Matrix Factorization (PMF) models (Paatero and Tapper, 1994, Paatero, 1997)  
27 have been widely used to identify and quantify sources of VOCs, generally in urban  
28 environments (e.g. Latella et al., 2005, Leuchner and Rappenglück, 2010, Gaimoz et al., 2011,  
29 Yuan et al., 2012). This type of analysis allows the separation of different sources (e.g.  
30 vehicular exhaust, fuel evaporation, residential heating etc...) and the apportionment of those  
31 sources to the VOC budget. PMF was also used at remote sites (Lanz et al., 2009, Sauvage et  
32 al., 2009, Leuchner et al., 2015), despite the need of assuming mass conservation between the  
33 source location and the measurement site in this approach (Hopke et al., 2003). In such  
34 environments, PMF can be used as a tool to identify aged primary sources as well as



1 photochemical formation of organic trace gases. This approach can, therefore, be useful to get  
2 insights into the sources and processes involved in the evolution of organic trace gases  
3 measured at remote locations. For example, Leuchner et al. (2015) applied the PMF to 24 C<sub>2</sub>-  
4 C<sub>8</sub> Non Methane HydroCarbons (NMHCs) measured at a remote site at Hohenpeissenberg  
5 (980 m asl). These authors obtained 6 different factors assigned to primary biogenic  
6 emissions, short-lived combustion, short- and long-lived evaporative emissions, residential  
7 heating, and a background component.

8 Similar PMF approaches are also conducted on the organic fraction of aerosols  
9 measured mostly by Aerosol Mass Spectrometers (AMS) to identify different components  
10 characterized by their sources, their way of formation and/or their chemical composition (Ng  
11 et al., 2010a, Zhang et al., 2011). For example, aerosol factors such as HOA (Hydrocarbon-  
12 like Organic Aerosol), and OOA (Oxygenated-like Organic Aerosol) are commonly extracted  
13 from AMS spectra using PMF analysis and are attributed to POA and SOA respectively  
14 (Zhang et al., 2011). The latter can also be separated into several factors as a function of the  
15 volatility: Low-Volatile-OOA (LV-OOA) and Semi-Volatile-OOA (SV-OOA) (Zhang et al.,  
16 2011). For example, Hildebrandt et al. (2010) detected two types of OOA with low volatility  
17 using PMF on AMS data recorded at Finokalia, an eastern Mediterranean remote site, while  
18 no HOA was present in detectable amounts. On the contrary, PMF analysis applied on aerosol  
19 measurements performed at an urban background site in Barcelona in spring, in the western  
20 Mediterranean basin, revealed a significant impact of local primary emissions with  
21 Hydrocarbon Organic Aerosol, Cooking Organic Aerosol and Biomass Burning Organic  
22 Aerosol factors accounting for 44% of OA, although regional and local secondary sources  
23 (LV-OOA and SV-OOA) dominated the OA burden (Mohr et al., 2012). Another study,  
24 combining ACSM measurements and <sup>14</sup>C analysis, conducted in Barcelona in summer 2013,  
25 revealed a large contribution of anthropogenic sources for this environment with fossil OC  
26 representing 46% to 57% of total OA. However, a larger contribution of secondary origin for  
27 fossil OC (>70%) and non-fossil OC (37-60%) was observed, leading to a large fraction of  
28 OA contained in OOA factors (Minguillon et al., 2016). Macro-tracer analysis represents an  
29 alternative solution to apportion OA and can be used to allocate/verify specific OA factors  
30 derived from PMF analysis. For instance, in atmospheres not impacted by biomass burning,  
31 water-soluble organic compounds (WSOC) have shown to provide valuable information on  
32 SOA that could be mainly of biogenic origin (Sullivan et al., 2004, 2006; Heald et al., 2006;  
33 Miyazaki et al., 2006; Kondo et al., 2007; Weber et al., 2007; Hennigan et al., 2008b).



1 More recently, combined source apportionments of organic aerosol and VOCs were  
2 performed in urban environments (Slowik et al., 2010; Crippa et al., 2013a), allowing a better  
3 classification of organic aerosol (OA) from the PMF analysis. This type of analysis also  
4 allowed getting insights into OA sources such as the identification of gaseous precursors.

5 Residential time analysis allow the geographical location of potential source areas by  
6 combining measured or estimated variables at a receptor site with back-trajectory analyses  
7 (Ashbaugh et al., 1985; Seibert et al., 1994; Stohl, 1996). Combined with PMF results, these  
8 models have been used to locate source regions of the PMF factors (Hwang and Hopke, 2007;  
9 Lanz et al., 2009; Tian et al., 2013). This association of receptor-oriented models can be  
10 powerful to identify the nature of the source or the chemical processes characterizing the PMF  
11 factors. The Concentration Field (CF) is one of these source-receptor inverse models, which  
12 was developed by Seibert et al. (1994). It consists in a redistribution of the measured or  
13 estimated variables in grid cells along estimated back-trajectories.

14 The Mediterranean basin is an ideal location to study the sources and the fate of organic  
15 carbon during long range transport since it is impacted by strong natural and anthropogenic  
16 emissions and undergoes intense photochemical events (Lelieveld et al., 2002). The  
17 ChArMEx project (Chemistry-Aerosol Mediterranean Experiment) aims at assessing the  
18 present and future state of the atmospheric environment and of its impacts in the  
19 Mediterranean basin. This initiative proposes to set up a coordinated experimental effort for  
20 an assessment of the regional budgets of tropospheric trace species, of their trends, and of  
21 their impacts on air quality, marine biogeochemistry, and regional climate. For that purpose an  
22 intensive field campaign was performed during the summer 2013, at Cape Corsica (North of  
23 Corsica Island) where a full suite of trace gases and aerosol species were measured for 3  
24 weeks. In the framework of ChArMEx, the CARBOSOR (CARBON within continental  
25 pollution plumes: SOurces and Reactivity) project aimed more specifically at investigating the  
26 sources of primary and secondary organic trace gases, as well as the composition of  
27 continental plumes reaching Cape Corsica, with the goal of assessing their impacts on the  
28 photo-oxidants and/or SOA sources and levels.

29 As part of the ChArMEx and CARBOSOR projects, this study investigates the  
30 composition, the sources and the chemistry of atmospheric organic matter by combining  
31 different statistical tools, i.e. the PMF, ME-2 (Multilinear Engine-2) models and the  
32 Concentration Field method. This approach was used to (i) identify co-variation factors of  
33 measured VOCs that are representative of primary emissions at various stages of ageing and  
34 chemical transformations occurring during long range transport, and to (ii) better characterize



1 the different fractions of organic aerosol. The PMF factors were then used to assess the origin  
2 of non-refractive organic species in PM<sub>1</sub> (Particulate Matter with aerodynamic diameter  
3 below 1 μm) observed at the measurement site, and especially to try to determine the fraction  
4 of biogenic versus anthropogenic OA.

5

## 6 **2 The ChArMEx experiment**

7

### 8 **2.1 Description of the Cape Corsica ground site**

9

10 The ChArMEx SOP2 (Short Observation Period 2) field campaign took place from 15  
11 July to 05 August 2013. The measurement site is located at Ersa in Cape Corsica (42.969°N,  
12 9.380°E), at the top of a hill (alt 533 m above sea level, asl), a few kilometres away from the  
13 sea in all directions (6, 4.5, and 2.5 km from the east, north and west sides respectively) (see  
14 Figure 1). The measurement site is surrounded by widespread vegetation such as “maquis”  
15 shrub-land typical of Mediterranean areas (Zannoni et al., 2015). The closest city, Bastia, is  
16 located approximately 30 km south of the site. It is the second largest city in Corsica (44 121  
17 inhabitants, census 2012), which hosts the main harbour of the island with about 413 000 and  
18 614 000 passengers in July and August 2013, respectively (CCI Territorial Bastia Haute  
19 Corse, 2013). However, the Cape Corsica peninsula is characterized by a mountain range  
20 (peaking between 1,000 and 1,500m asl), which acts as a natural barrier isolating the  
21 measurement site from any atmospheric flow originating from Bastia.

22

### 23 **2.2 VOC measurements**

24

25 During the ChArMEx SOP2 field campaign more than 80 VOCs, including Non-  
26 Methane HydroCarbons (NMHCs) and Oxygenated (O)VOCs, were measured using  
27 complementary online and offline techniques whose sampling inlets were located  
28 approximately 1.5 m above the roof of a trailer where the instruments were housed. Table 1  
29 summarizes the VOCs measurement performed during the campaign.

30

31 Sixteen (16) protonated masses were extracted from the Proton Transfer Reaction-  
32 Time of Flight Mass Spectrometer (PTR-ToF-MS, KORE Inc<sup>®</sup> 2<sup>nd</sup> generation) leading to the  
32 measurements of OVOCs (alcohols such as methanol: m/z 33.03, aldehydes and ketones,  
33 carboxylic acids), aromatics (sum of both C-8 and C-9 aromatics: m/z 107.09 and m/z 121.10,  
34 respectively) and biogenic VOCs (BVOCs such as isoprene: m/z 69.07 and the sum of



1 monoterpenes:  $m/z$  137.13). Ambient air was sampled through a 5-m long PFA line  
 2 (PerFluoroAlkoxy, 1/4"-o.d.) held at 50°C using a constant flow rate of 1.2 L min<sup>-1</sup> to  
 3 minimize the residence time to 4 s. The PTR-ToF-MS sampling flow rate was set at  
 4 150 mL min<sup>-1</sup> and an additional pump was used to raise the flow rate to the required 1.2  
 5 L min<sup>-1</sup> in the sampling line. The instrument was operated at reactor pressure and temperature  
 6 of 1.33 mbar and 40°C, respectively, leading to an E/N ratio of 135 Td.

7 An automated zero procedure was performed every hour for 10 min. Humid zero air  
 8 was generated by passing ambient air through a catalytic converter (stainless steel tubing  
 9 filled with Pt wool held at 350°C) allowing to get the same relative humidity than in ambient  
 10 air. During the campaign, the PTR-ToF-MS was calibrated every three days using a Gas  
 11 Calibration Unit (IONICON<sup>®</sup>) and various standards including a mix of 15 VOCs (including  
 12 NMHCs, OVOCs and Chlorinated VOCs) in a canister (Restek<sup>®</sup>), a mix of 9 NMHCs in a  
 13 second cylinder (Praxair<sup>®</sup>) and a mix of 9 OVOCs in a cylinder (Praxair<sup>®</sup>) (see supplementary  
 14 material Table S1). Additional calibrations were performed before and after the campaign  
 15 using permeation tubes (Kin-Tec Inc<sup>®</sup>) for carboxylic acids and a Liquid Calibration Unit  
 16 (IONICON<sup>®</sup>) with a certified solution for methylglyoxal. To account for a possible drift of the  
 17 PTR-ToF-MS sensitivity during the campaign, relative calibration factors were determined for  
 18 the carboxylic acids and methyl glyoxal using a specific VOC as a reference (present in the  
 19 standard mixtures used to calibrate the PTR-ToFMS during the campaign and with a  $m/z$   
 20 value as close as possible for each compound: e.g. acetaldehyde, acetone and  
 21 methylethylketone for formic acid, acetic acid, and methylglyoxal, respectively).

22 Signal of every unit mass is accumulated over 10 min and normalized by the signals of  
 23 H<sub>3</sub>O<sup>+</sup> and the first water cluster H<sub>3</sub>O<sup>+</sup>(H<sub>2</sub>O) as proposed by de Gouw and Warneke (2007).  
 24 Concentrations are calculated using Eq. (1):

$$[X] = \frac{i_{X\_net}}{(i_{H_3O^+} + X_r \cdot i_{H_3O^+(H_2O)})} \cdot \frac{150000}{R_{f,X}} \quad (1)$$

25 Where [X] represents the mixing ratio of a given VOC,  $i_{X\_net}$  the net signal recorded for  
 26 this VOC,  $i_{H_3O^+}$  and  $i_{H_3O^+(H_2O)}$  the signals of H<sub>3</sub>O<sup>+</sup> and H<sub>3</sub>O<sup>+</sup>(H<sub>2</sub>O) at  $m/z$  19 and 37, but  
 27 respectively recorded at  $m/z$  21 and 39, to avoid any saturation of the detector at  $m/z$  19 and  
 28 37, and recalculated using the isotopic ratio between <sup>16</sup>O and <sup>18</sup>O.  $X_r$  is a factor introduced to  
 29 account for the effect of humidity on the PTR-ToFMS sensitivity (de Gouw and Warneke,  
 30 2007) and determined experimentally through calibrations performed at various relative  
 31 humidities.  $R_{f,X}$  is the sensitivity determined during calibration experiments (in ncts ppt<sup>-1</sup>) and



1 normalized to 150000 counts  $s^{-1}$  of  $H_3O^+$  ions. The latter is the number of counts of reagent  
2 ions observed in our PTR-ToFMS instrument.

3 Forty-three (43)  $C_2$ - $C_{12}$  NMHCs, including alkanes, alkenes, alkynes and aromatics,  
4 were measured using an online Gas Chromatograph (GC) equipped with two columns and a  
5 dual Flame Ionization Detection (FID-FID) system (Perkin Elmer<sup>®</sup>). This instrument has been  
6 previously described in detail by Badol et al. (2004). Briefly, air is sampled via a 5-m length  
7 PFA line (1/8"-o.d.) at a flow rate of 15 mL  $min^{-1}$ . Ambient air passes through a Nafion  
8 membrane to dry it and is then pre-concentrated during 40 min onto a sorbent trap made of  
9 Carboxpack B and Carboxieve SIII and held at  $-30^\circ C$  by a Peltier cooling system. The trap is  
10 then heated up to 300  $^\circ C$  (40  $^\circ C s^{-1}$ ) to desorb and inject VOCs in a Perkin Elmer GC system.  
11 The chromatographic separation is performed using two capillary columns thanks to a  
12 switching facility. This approach allows for a better separation and reduces co-elution issues  
13 (Badol et al., 2004). The first column designed for  $C_6$ - $C_{12}$  compounds is a CP Sil 5CB  
14 (50 m $\times$ 0.25 mm $\times$ 1  $\mu m$ ), while the second column designed for the  $C_2$ - $C_5$  compounds is a plot  
15  $Al_2O_3/Na_2SO_4$  (50 m $\times$ 0.32 mm $\times$ 5  $\mu m$ ). The separation step lasts 50 min, leading to a total  
16 time resolution of 1h30'. Finally, eluted compounds are detected using the 2 FID detectors.  
17 Calibrations were performed at the beginning, at the middle and at the end of the campaign,  
18 using a standard mixture containing 32 compounds (NPL<sup>®</sup>, see supplementary material Table  
19 S2).

20 Sixteen (16)  $C_3$ - $C_7$  OVOCs, including aldehydes, ketones, alcohols, ethers, esters, as  
21 well as 6 NMHCs, including BVOCs and aromatics, were measured using an online GC/FID-  
22 Mass Spectrometer (MS). This instrument has been described in details by Roukos et al.  
23 (2009). Ambient air is sampled via a 5-m length PFA line (1/8") at a flow rate of 15 mL  $min^{-1}$   
24 by an air server unit (Markes International<sup>®</sup>, Unity I) and passes through a KI ozone scrubber.  
25 The sampled air is pre-diluted (50% dilution) with dry zero air to keep the relative humidity  
26 below 50%. A sample is then collected into an internal trap cooled by a Peltier system at  
27 12.5  $^\circ C$  and consists in a 1.9 mm i.d. quartz tube filled with two different sorbents (5 mg of  
28 Carboxpack B and 75 mg of Carboxpack X, Supelco<sup>®</sup>). Compounds trapped onto the sorbents  
29 are then thermally desorbed at 280  $^\circ C$  and injected into the column and analyzed by a GC  
30 (Agilent<sup>®</sup>) equipped with a FID for quantification and a Mass Spectrometer (MS) to help with  
31 the identification. The thermodesorbed compounds are passed through a high polar CP-lowox  
32 column (30 m $\times$ 0.53 mm $\times$  10  $\mu m$ , Varian<sup>®</sup>) for separation. The sampling and analysis steps  
33 last 40 and 50 min, respectively, for a total time resolution of 1h30'. Calibrations were



1 performed several times during the campaign, using a standard mixture containing 29  
2 compounds (Praxair<sup>®</sup>, see supplementary material Table S2).

3 Thirty-five (35) C<sub>5</sub>-C<sub>16</sub> NMHCs, including alkanes, alkenes, aromatics and BVOCs, as  
4 well as 5 C<sub>6</sub>-C<sub>12</sub> n-aldehydes were collected by active sampling into sorbent cartridges using  
5 an Automatic Clean Room Sampling System (ACROSS-TERA Environment<sup>®</sup>) and were  
6 analyzed later by GC-FID. This technique has already been described by Detournay et al.  
7 (2011) and its set-up in the field was discussed by Ait-Helal et al. (2014). Briefly, air was  
8 sampled via a 3-m length PFA line (1/4"-o.d.) at 200 mL min<sup>-1</sup> and was passed through a  
9 MnO<sub>2</sub> ozone scrubber and a stainless-steel particle filter (2µm pore size diameter). VOCs are  
10 collected during 3 h in cartridges filled with Carbopack C (200 mg) and Carbopack B  
11 (200 mg), formerly conditioned with purified air at 250 °C during 24 h.

12 Finally, sixteen (16) C<sub>1</sub>-C<sub>8</sub> carbonyl compounds were collected offline during 3 h using  
13 the same sampling device than for solid-sorbent cartridges by active sampling on  
14 DiNitroPhenylHydrazine (DNPH) cartridges (Waters<sup>®</sup>). These compounds were analyzed  
15 later by High Performance Liquid Chromatography (HPLC) with UV detection. Air was  
16 sampled via a 3-m length PFA line (1/4"-o.d.) at 1.5 L min<sup>-1</sup> and was passed through a KI  
17 ozone scrubber and a stainless-steel particle filter (2µm pore size diameter). Data are available  
18 only for the first 10 days of the campaign (15/07-25/07) due to unresolved leakage issues for  
19 the rest of the campaign and hence a contamination of the cartridges with indoor air from the  
20 trailer was suspected.

21 The detection limits for each species measured by all five techniques were determined  
22 as 3σ of the blank variation for PTR-ToF-MS and offline sampling methods and as 3σ of the  
23 baseline fluctuations for online GCs. The uncertainties for each species were estimated  
24 following the "Aerosols, Clouds, and Trace gases Research InfraStructure network"  
25 (ACTRIS) guidelines for uncertainty evaluation (ACTRIS Measurement Guideline VOC,  
26 2012), taking into account precision, detection limit and systematic errors of the  
27 measurements. The range of uncertainties and detection limits for each technique is given in  
28 Table 1. Furthermore, systematic intercomparisons for compounds measured by different  
29 techniques (e.g. isoprene, monoterpenes, acetone, n-pentane, benzene, etc...) were performed  
30 to validate the database (not shown).

31

### 32 **2.3 Ancillary gas measurements**

33



1 During the campaign, measurements of other trace gases (NO, NO<sub>2</sub>, O<sub>3</sub>, CO, CO<sub>2</sub>, CH<sub>4</sub>,  
2 H<sub>2</sub>O, SO<sub>2</sub>) were additionally performed at the same measurement site.

3 NO and NO<sub>2</sub> were measured by a commercial analyzer (CRANOX II, EcoPhysics®)  
4 using ozone chemiluminescence with a time resolution of 5 min. Since this technique allows  
5 the direct measurements of NO only, NO<sub>2</sub> was converted into NO using a photolytic converter  
6 incorporated in the analyzer.

7 O<sub>3</sub> was measured using a UV absorption analyzer (TEI 49i, Thermo Environmental  
8 Instrument Inc®) at a time resolution of 5 min. CO, CO<sub>2</sub>, CH<sub>4</sub>, H<sub>2</sub>O were simultaneously  
9 measured by a commercial analyzer (G2401, PICARRO®) based on Cavity Ring Down  
10 Spectroscopy (CRDS). Finally, SO<sub>2</sub> was measured by a commercial analyzer (TEI 43i,  
11 Thermo Environmental Instrument Inc®) using fluorescence spectroscopy at a time resolution  
12 of 5 min.

13

## 14 **2.4 Aerosol measurements**

15

16 Online measurements of organic aerosols (PILS-IC, PILS-TOC, OCEC Sunset Field  
17 Instruments, Q-ACSM) have been available since beginning of June 2013, but data reported  
18 here are restricted to the ChArMEx SOP2 period (15/07-05/08/2013) for which VOC  
19 measurements have been performed.

20 In addition, Black carbon (BC) has been continuously monitored, during the same  
21 extended period, using a 7-wavelength aethalometer model AE-31 (MAGEE Scientific®) at a  
22 time resolution of 15 min.

23

### 24 **2.4.1. PILS-IC instrument**

25

26 Measurements of major anions (Cl<sup>-</sup>, NO<sub>3</sub><sup>-</sup>, SO<sub>4</sub><sup>2-</sup>), cations (Na<sup>+</sup>, NH<sub>4</sub><sup>+</sup>, K<sup>+</sup>, Mg<sup>2+</sup>, Ca<sup>2+</sup>)  
27 and light organics (methanesulfonate (MSA), oxalate) in PM<sub>10</sub> were performed using a  
28 Particle-into-Liquid-Sampler (PILS; Orsini et al., 2003) running at 11.8±0.5 L min<sup>-1</sup> and  
29 coupled with two Ion Chromatographs (IC). More details on the settings of the PILS-IC can  
30 be found in Sciare et al. (2011). During this field campaign, ambient concentrations of ions  
31 were corrected from blanks performed every day for 1h and achieved by placing a total filter  
32 upstream of the sampling system. Very low blank values (typically below 1 ppb) were  
33 systematically detected for all ions providing further confidence on the efficiency of the  
34 acidic/basic denuders set upstream of the PILS, the lack of contaminants in our system, and



1 the quality of our Milli-Q water during the whole duration of the study. Liquid flow rates of  
2 the PILS were delivered by peristaltic pumps and set to  $1.0 \text{ ml min}^{-1}$  for producing steam  
3 inside the PILS and  $0.37 \pm 0.02 \text{ ml min}^{-1}$  for rinsing the impactor. Calibrations (5 to 7 points)  
4 of anions and cations (including light organics) were performed every two weeks (from end of  
5 May 2013 to beginning of August 2013) with no significant drift reported (e.g. below 5%  
6 difference on average). Based on IC settings, the detection limit ( $2\sigma$ ) for ions was typically  
7  $0.1 \text{ ppb}$ , which corresponds to an atmospheric concentration of  $\sim 1 \text{ ng m}^{-3}$ . The overall  
8 uncertainty associated with PILS-IC measurements includes variability in air sampling flow  
9 rate, liquid flow rate, calibration, and collection efficiency and was estimated to be of the  
10 order of 25%. Time resolutions were typically of 24 min for anions (including light organics)  
11 and 12 min for cations. Because this study focuses on organics in the atmosphere, only MSA  
12 and oxalate data will be presented and discussed here. A total of 761 and 996 valid data points  
13 of MSA and Oxalate were obtained, respectively, with concentrations ranging for MSA from  
14  $4 \text{ to } 59 \text{ ng m}^{-3}$  ( $21 \text{ ng m}^{-3}$  on average) and ranging for oxalate from  $1 \text{ to } 24 \text{ ng m}^{-3}$  ( $10 \text{ ng m}^{-3}$   
15 on average).

16

#### 17 **2.4.2. PILS-TOC instrument**

18

19 Measurements of water-soluble organic compounds (WSOC) in  $\text{PM}_{10}$  were performed  
20 every 4 min using a modified Particle-into-Liquid-Sampler (Brechtel Manufacturing Inc.,  
21 USA; Sorooshian et al., 2006) coupled with a total organic carbon analyzer (TOC, Model  
22 Sievers 900, Ionics Ltd, USA). More information on the operation procedure of this  
23 instrument is provided by Sciare et al. (2011). Briefly, the PILS-TOC instrument is running at  
24  $15 \text{ L min}^{-1}$  and a measured dilution factor of 1.30 was taken in the instrument which is close  
25 to the one reported by Sullivan et al. (2006). A polyethylene filter of  $0.45 \mu\text{m}$  pore size  
26 diameter was set in-line in the aerosol liquid flow (downstream of the PILS collector) in order  
27 to analyze solely the water-soluble OC fraction. Daily blanks for the PILS-TOC instrument  
28 were achieved by placing a total filter upstream of the sampling system for 1h. In this  
29 configuration, approximately 15 min were necessary to reach blank values which were very  
30 stable during the campaign showing a mean concentration of  $35.6 \pm 2.6 \text{ ppbC}$ , very similar to  
31 the one reported by Sciare et al. (2011). Note that most of the blank concentration refers to the  
32 TOC concentration in the ultra-pure water used in the PILS instrument (typically  $25 \text{ ppbC}$ ),  
33 suggesting little contamination in the PILS instrument as well as a good efficiency of the  
34 VOC denuder placed upstream. Note also that the daily blanks for the PILS-TOC instrument



1 were performed at different hours of the day and did not show a clear diurnal pattern that  
2 could be linked to diurnal variations of VOCs. Ambient WSOC measurements were then  
3 corrected from this blank value. Limit of quantification of ambient WSOC measurements was  
4 estimated as  $2\sigma$  (twice the uncertainty calculated for the blank concentrations), corresponding  
5 to about  $0.48 \mu\text{gC m}^{-3}$ . A total of 6592 valid data points were collected during the period of  
6 the study (15/07-05/08/2013), corresponding to a mean ambient (blank corrected) WSOC  
7 concentration of  $11.6 \pm 6.7 \text{ ppbC}$  (i.e.  $1.00 \pm 0.60 \mu\text{gC m}^{-3}$ ).

8

### 9 **2.4.3. OCEC Sunset Field instrument**

10

11 Semi-continuous (2-h time resolution) concentrations of elemental carbon (EC) and  
12 organic carbon (OC) in  $\text{PM}_{2.5}$  were obtained in the field from an OCEC Sunset field  
13 instrument (Sunset Laboratory, Forest Grove, OR, USA; Bae et al., 2004) running at  $8 \text{ L min}^{-1}$   
14 <sup>1</sup>. A denuder provided by the manufacturer was set upstream in order to remove possible  
15 adsorption of VOCs onto the filter used to collect fine aerosols in the instrument.  
16 Measurement uncertainty given by the OCEC Sunset field instrument is poorly described in  
17 literature and an estimate of 20% for this uncertainty was taken here following Peltier et al.  
18 (2007). This instrument has been running continuously for the whole duration of the  
19 campaign (15/07-05/08/2013) with 252 valid EC and OC data points obtained.

20

### 21 **2.4.4. Q-ACSM instrument**

22

23 Since summer 2012, measurements of the chemical composition of non-refractory  
24 submicron aerosol ( $\text{NR-PM}_1$ ) have been carried out at the measurement site using a  
25 Quadrupole Aerosol Chemical Speciation Monitor (Q-ACSM, Aerodyne Research Inc.  
26 Billerica, MA). This recently developed instrument shares the same general structure with the  
27 Aerosol Mass Spectrometer (AMS) but has been specifically developed for long-term  
28 monitoring. An exhaustive description of ACSM is available in Ng et al. (2011) while a  
29 growing number of studies have already reported long-term observations of  $\text{NR-PM}_1$   
30 composition and concentrations using it (Ripoll et al., 2015; Minguillón et al., 2015; Petit et  
31 al., 2015; Parworth et al., 2015; Budisulistiorini et al., 2015).

32 The Q-ACSM instrument used here participated to the large intercomparison study of  
33 13 Q-ACSM that took place at the ACMCC (Aerosol Chemical Monitor Calibration Center;  
34 <https://acmcc.lscce.ipsl.fr/>), three months after this field campaign and showed - for



1 atmospheric concentrations and fragmentation pattern - very consistent results in terms of  
2 reproducibility and consistency (Crenn et al., 2015). Source apportionment performed with  
3 the same Q-ACSM (during the intercomparison study at ACMCC) has also led to very  
4 consistent and comparable results (Frölich et al., 2015). The calibration of this instrument  
5 with mono-dispersed (300 nm diameter) ammonium nitrate particles was performed at  
6 ACMCC in May 2013, about two months before the start of this study. Because ambient air  
7 was dried by a Nafion membrane before entering into the Q-ACSM and because ammonium  
8 nitrate was not significant during the field campaign, we have kept here a constant collection  
9 efficiency (CE) of 0.5. Onsite atmospheric concentrations delivered by the Q-ACSM were  
10 consistent for NR-PM<sub>1</sub> and SO<sub>4</sub> concentrations obtained with co-located online instruments  
11 (Scanning Mobility Particle Sizer and Particle-Into-Liquid-Sampled-Ion-Chromatograph).  
12 The Q-ACSM instrument has been continuously operating for the whole duration of the  
13 campaign (15/07-05/08/2013), with a total of 1148 valid data points of 30 min time resolution  
14 each.

15

## 16 **2.5 Back-trajectory classification**

17

18 A study of back-trajectories was performed to identify and classify the origin and  
19 typology of the different air masses reaching Cape Corsica during the campaign and to  
20 support interpretation of the results. Back-trajectories of 48 h were calculated, every 6 h  
21 during the whole campaign, with an ending point at the measurement site (42.969°N, 9.380°E,  
22 alt: 600 m asl) using the online version of the HYSPLIT (HYbrid Single-Particle Lagrangian  
23 Integrated Trajectory) model developed by the National Oceanic and Atmosphere  
24 Administration (NOAA) Air Resources Laboratory (ARL) (Draxler and Hess, 1998; Stein et  
25 al., 2015). This model was chosen for its easy and quick visualisation facility.

26 A visual classification of these back-trajectories was performed as a function of their  
27 origin, altitude and wind speed and segregated into five clusters (Figure 2). A description of  
28 the 5 clusters is provided in Table 2. Four clusters correspond to different wind sectors  
29 defined by the origin of the air masses reaching the measurement site (West, North-East,  
30 South and North-West). These clusters are characterized by different transit times since the  
31 last potential anthropogenic contamination (i.e. since the air mass left the continental coasts).  
32 Indeed, the air masses from the “Marine-West” cluster have spent 36 to more than 48 h above  
33 the sea, while they have spent 10-20 h and 12-18 h for the “Europe-North-East”, and the  
34 “France-North-West” clusters respectively (Table 2). For the “Corsica-South” cluster, the



1 indicated transit time (12-24 h) considers the time spent by air masses above land (Corsica  
2 and Sardinia Islands) before passing over the sea. These different transit times potentially  
3 indicate different atmospheric processing times for the air masses, the longest being for the  
4 “Marine-West” cluster.

5 The last cluster gathers air masses transported over short distances over 48 h and  
6 therefore during calm situations with low wind speed (Figure 2). The “Calm-Low Wind”  
7 cluster and the “Marine-West” cluster are the two most representative clusters, representing  
8 each 30% of the air masses origin. They are followed by the “Europe-North-East” cluster  
9 representing 26%, and then by the “Corsica-South” and “France-North West” representing  
10 8% and 6% of the air mass origins, respectively.

11

## 12 **2.6 Photochemical age of air masses**

13

14 Regarding the relative long transit time of air masses travelling from continental source  
15 areas to the measurement site (from 10 to more than 48 h, see section 2.5), the assessment of  
16 the photochemical age using the field observations can be performed with specific ratios of  
17 long-lived VOCs measured at significant levels at the site. The use of graphic representations  
18 of the ratios of three different alkanes, such as  $\ln(\text{butane/ethane})$  vs  $\ln(\text{propane/ethane})$  is well  
19 suited to assess the photochemical age of air masses which experienced long-range transport  
20 (Rudolph and Johnen, 1990; Jobson et al., 1994; Parrish et al., 2007). Considering an air  
21 parcel isolated from any new emission or mixing with other air parcels, and considering that  
22 the main loss of alkanes is their oxidation by the OH radical; one can estimate the relation of  
23 three alkanes as described by eq. (2) (Jobson et al., 1994).

$$14 \quad \ln \frac{[\text{butane}]}{[\text{ethane}]} = \frac{k_{\text{butane}} - k_{\text{ethane}}}{k_{\text{propane}} - k_{\text{ethane}}} \ln \frac{[\text{propane}]}{[\text{ethane}]} + \beta \quad (2)$$

24  $k_i$  is the bimolecular reaction rate constant of the reaction between the specie  $i$  and OH.  
25 The  $\beta$  parameter depends on the emission ratios of these three species and the reaction rate  
26 constants.

27 Since ethane is the less reactive of these compounds, the ratios will tend to decrease  
28 with increasing photochemical age. The evolution of  $\ln(\text{butane/ethane})$  as a function of  
29  $\ln(\text{propane/ethane})$  during the ChArMEx SOP2 field campaign in Cape Corsica is presented  
30 in Figure 3. The points of Figure 3 have been colour-coded as a function of the back-  
31 trajectory clusters described in the previous section.



1           Figure 3 reveals that the air masses of the Marine West (light blue) cluster present  
2 higher photochemical ages (lower alkane ratios) relatively to the air masses of the European-  
3 North-East (purple) cluster, consistent with the analysis of back-trajectories (c.f. section 2.5).  
4 Moreover, the good linearity observed in the evolution of the ratios allows the qualitative  
5 comparison of the photochemical age of air masses from the different wind clusters.

6           These ratios have been compared to ratios observed at measurement sites of different  
7 types (see Supplementary Material Fig. S3). The ratios obtained during the campaign cover a  
8 large range of values with, in particular, very low values for the Marine-West cluster, typical  
9 of relatively aged air masses sampled at very remote sites. It indicates that air masses can  
10 spend several days over the sea before reaching the measurement site especially for the  
11 Marine-West cluster. In general, ratios representative of remote locations are observed all  
12 along the campaign, confirming the remote nature of the Cape Corsica station.

13           It is noteworthy that the slope observed for our dataset (0.65, see Figure 3) is  
14 significantly lower than the theoretical ones calculated for an isolated air mass experiencing a  
15 selective oxidation by OH (2.50) or by Cl (1.97). The lack of concordance with theoretical  
16 slopes has often been observed (e.g. Parrish et al., 1992; McKeen et al., 1996) and has been  
17 attributed to the mixing between air parcels of different histories and origins during long-  
18 range transport (Parrish et al., 2007 and references therein).

19

### 20 **3 Source-receptor models**

21

#### 22 **3.1 The Positive Matrix Factorization (PMF)**

23

24           In this study, US E.P.A PMF 3.0 was used to perform the factor analysis. For a  
25 detailed presentation of the PMF principle, the reader can refer to the first description made  
26 by Paatero and Tapper (1994) and to the user's guide written by Hopke (2000). Briefly, a  
27 specific dataset at a receptor site can be viewed as a data matrix  $X$  containing  $i$  samples and  $j$   
28 measured chemical species. The PMF identifies the number of factors  $p$ , i.e. the number of  
29 emission sources and/or chemical processes, driving ambient concentrations of the measured  
30 species. It, therefore, allows decomposing the matrix  $X$  into a product of two matrices: the  
31 species profile ( $f$ ) of each source with a dimension of  $p \times j$  (representing the repartition of each  
32 measured chemical species in the factors); the contribution ( $g$ ) of each factor to each sample  
33 with a dimension of  $i \times p$  (representing the time evolution of each factor); and allows  
34 minimizing the residual error  $e$ . This is summarized in eq. (3):



$$X_{ij} = \sum_{k=1}^p g_{ik} \times f_{kj} + e_{ij} \quad (3)$$

1 The minimization of the residual sum of squares Q is performed using eq. (4) to derive  
 2 the solution of eq. (3).

$$Q = \sum_{i=1}^n \sum_{j=1}^m \frac{e_{ij}^2}{s_{ij}^2} = \sum_{i=1}^n \sum_{j=1}^m \left[ \frac{X_{ij} - \sum_{k=1}^p g_{ik} \times f_{kj}}{s_{ij}} \right]^2 \quad (4)$$

3 Where  $S_{ij}$  is the uncertainty matrix associated to the data matrix  $X_{ij}$ , estimated as  
 4 described in section 2.2.

5 The PMF analysis was conducted on a dataset of 42 species, including NMHCs, and  
 6 OVOCs measured by the two online GCs and the PTR-ToFMS, and 329 observations, the  
 7 time resolution being 1h30' (time resolution of the GCs). Measurements by active sampling  
 8 on sorbent and DNPH cartridges were not included in this dataset due to their low time  
 9 resolution (3h), which would have resulted in too few observations. Furthermore, compounds  
 10 were not considered when missing, when more than half of observations were below the  
 11 detection limit, or when associated to a low signal-to-noise ratio ( $s/n < 1$  in our case). Missing  
 12 values and values below the detection limit in the selected dataset were replaced by the  
 13 geometric mean and half of the detection limit, respectively, following the method used by  
 14 Sauvage et al. (2009). To minimize the weight of these observations in the PMF results, the  
 15 uncertainties of missing values and values below the detection limit were set to 4 times the  
 16 geometric mean and 5/6 of the detection limit, respectively. PMF also allows the  
 17 minimization of the contribution of species of low signal-to-noise ratio ( $s/n < 1.5$  in our case)  
 18 by declaring these species as “weak” and hence tripling their original uncertainties. Fourteen  
 19 species have been declared as “weak” in this work.

20 Ethane, methanol and acetone are characterized by high background concentrations at  
 21 the measurement site. To minimize the weight of these three species in the PMF results, their  
 22 estimated background concentrations (500, 1000 and 1200 ppt for ethane, methanol and  
 23 acetone, respectively) were subtracted to the measured concentrations in the data matrix X.  
 24 These values were chosen arbitrarily to subtract the background concentrations of these  
 25 species keeping their variability and avoiding near zero values.

26 The PMF was run following the protocol proposed by Sauvage et al. (2009) and lying  
 27 on several statistical indicators (unexplained part for each factors, correlation between the  
 28 sum of the factor contributions and the sum of the measured concentration, the parameter Q  
 29 (see above), mean and standard deviation of scaled residuals ...) to determine the optimal



1 model parameters (number of factors, rotational parameter  $F_{\text{peak}}$ ) leading to the best solution.  
2 Based on this approach, we have derived a final solution with 6 factors for a  $F_{\text{peak}}$  of -0.5.

3 Moreover, the homogeneity of the database built using measurements from different  
4 techniques was studied to ensure that all instruments are well-represented in the solutions.  
5 This was done by checking that no substantial differences are observed between the scale  
6 residuals of the different instruments. We therefore calculated the mean of the absolute values

7 of scaled residuals for the three instruments  $\left( \frac{|e_{ij}|}{s_{ij}} \right)$  (0.73, 0.67 and 0.75 for the PTR-ToF-MS,

8 GC/FID-FID and GC/FID-MS, respectively). The differences observed between these  
9 parameters calculated for the three instruments are lower than 0.08. This indicates a  
10 reasonable homogeneity of the instrument databases (concentrations, uncertainties) since  
11 absolute differences below 0.25 have been determined to be satisfactory to avoid over-  
12 weighting of the measurements of a particular instrument in PMF solutions (Crippa et al.,  
13 2013a)). Therefore, no scaling procedure was performed on the database used in our PMF  
14 analysis.

15 Furthermore, 100 bootstrap runs were performed for the 6 factors solution to estimate  
16 the stability and uncertainty of this solution. This operation consisted in performing additional  
17 PMF runs using new input data files built by randomly selecting non-overlapping blocks of  
18 the original data matrix, the contribution of each factor derived from these runs being then  
19 compared to the original solution. The lowest correlation coefficient between bootstrap  
20 solutions and base run solutions was 0.6. The 6-factors solution appeared to be well-mapped  
21 in the base run with mapping of bootstrap factors to base run factors higher than 86% for all  
22 factors (see Supplementary material S4).

23

### 24 **3.2 Multilinear Engine (ME-2)**

25

26 Source apportionment of organic aerosol components from Q-ACSM was performed  
27 using Positive Matrix Factorization (PMF, Paatero, 1997; Paatero and Tapper, 1994) via the  
28 ME-2 solver (Paatero, 1999). An extended Q-ACSM dataset of 2 months (starting from 05/06  
29 till 5/08/2013) was used here in order to obtain a wider range of atmospheric variability and  
30 improve PMF output results. The extraction of OA data and error matrices as mass  
31 concentrations in  $\mu\text{g m}^{-3}$  over time, as well as their preparation for PMF/ME-2 according to  
32 Ulbrich et al. (2009), was done within the ACSM software, except for the down weighing



1 procedure of mass fragments which was performed using the interface source finder (SoFi,  
2 Canonaco et al., 2013), version 6.1. Only  $m/z$  up to 100 were considered here since they  
3 represented nearly the whole OA mass (around 98 %) and did not interfere with ion fragments  
4 originating from naphthalene. The interface SoFI was used to control ME-2 for the PMF runs  
5 of the ACSM OA data. Unconstrained PMF runs were investigated here with 1 to 6 factors  
6 and a moderate number of seeds (10) for each factor number without no conclusive results on  
7 the consistency of mass spectra profile obtained for the different factors. Constrained PMF  
8 runs have been investigated for that purpose with fixed factors for HOA (Hydrogen-like OA),  
9 with much more conclusive results and significant improvements compared to the  
10 unconstrained PMF. The results presented here were obtained using constrained PMF using  
11 an averaged HOA profile taken from Ng et al. (2010b) and constrained with a value of 0.1.  
12 The proper constrained PMF solution was selected based on the recommendations from  
13 Canonaco et al. (2013) (e.g. consistency of the factor profiles mass spectra, consistency of  
14 times series with external tracer, low  $Q/Q_{exp}$  value). These criteria are presented and  
15 discussed hereafter.

16

17 In this study, we therefore applied separate factorization analysis to both VOCs and  
18 aerosol databases. Another approach consists in a factorization analysis of combined aerosol  
19 and gaseous databases (Slowik et al., 2010; Crippa et al., 2013a). Thus, an attempt to perform  
20 such PMF analysis was conducted, using the gaseous database (42 VOCs) described above  
21 and full ACSM spectra as inputs and taking care of the homogeneity of the different inputs by  
22 applying a scaling procedure as proposed by Slowik et al. (2010) and Crippa et al. (2013a).  
23 However, it did not allow to satisfactorily apportion aerosol measurements and led to weaker  
24 solutions than the ME-2 analysis. It was therefore decided to keep separated solutions for both  
25 gas and aerosol phase organics.

26

### 27 **3.3 The Concentration Field model (CF)**

28

29 Receptor-oriented models have been developed to identify, localize and quantify  
30 potential source areas which impact the concentrations of a variable measured at a receptor  
31 site in the form of maps of a contribution quantity. In this study we have used the  
32 Concentration Field (CF) approach developed by Seibert et al. (1994). This method consists in  
33 redistributing concentrations of a variable observed at a receptor site along the back-  
34 trajectories, ending at this site, inside a predefined grid ( $0.5^\circ \times 0.5^\circ$ , for this study). The



1 calculated concentrations in each grid cells are weighted by the residence time that air parcels  
 2 spent in each cell following eq.

3 (5):

$$\log \bar{C}_{ij} = \frac{\sum_{L=1}^M (n_{ijL} \times \log C_L)}{\sum_{L=1}^M n_{ijL}} \quad (5)$$

4 Where  $C_{ij}$  is the calculated concentration of the  $ij$ -th grid cell,  $L$  the back-trajectory  
 5 index,  $M$  the total number of back-trajectories,  $C_L$  the concentration measured at the site when  
 6 the back-trajectory  $L$  reached it and  $n_{ijL}$  the number of points of the back-trajectory  $L$  which  
 7 fall in the  $ij^{\text{th}}$  grid cell. The latter is representative of the time spent by the back-trajectories in  
 8 the  $ij$ -th grid cell since a constant time step of 1 h is used between each point of a back-  
 9 trajectory.

10 The 3-day back-trajectories (selected to account for distant potential source areas of  
 11 species of long lifetimes), used in the CF analysis, were calculated by the British Atmospheric  
 12 Data Centre (BADC) model every hour. This model uses the wind fields calculated by the  
 13 European Centre for Medium-range Weather Forecasts (ECMWF) to determine the  
 14 trajectories of air masses. This model was selected here instead of Hysplit for convenience,  
 15 since format of output files matches the needed one for our CF model. Comparison of  
 16 randomly selected back-trajectories, in each identified clusters (see section 2.5), calculated by  
 17 both models (BADC and Hysplit) has revealed satisfactory agreement in terms of origin and  
 18 areas over-flown. The BADC back-trajectories were interrupted when the altitude of the air  
 19 mass exceeded 1500 m (asl), to get rid of the important dilution affecting air masses in the  
 20 free troposphere (the boundary layer height has been arbitrary set here to 1500 m (asl) for all  
 21 trajectories). Furthermore, the grid cells containing less than 5 trajectory points were not  
 22 considered for robustness purposes.

23 To take into account the uncertainties associated to the back-trajectories, a smoothing of  
 24 concentrations was applied to all the grid cells values as recommended by Charron et al.  
 25 (2000) and using eq. (6).

$$C_{ij-l} = \frac{\left( \sum_{p=1}^8 C_p + C_{ij} \right)}{9} \quad (6)$$



1           Where  $C_{ij-1}$  is the calculated concentration of the  $ij^{\text{th}}$  grid cell after smoothing,  $C_{ij}$  the  
2           calculated concentration of the grid cell before smoothing and  $C_p$  ( $1 < p < 8$ ) the concentrations  
3           before smoothing of the 8 neighbour grid cells.

4

## 5           **4 Results and Discussion**

6

### 7           **4.1 Overview of gaseous and aerosol measurement results**

8

#### 9           **4.1.1. Gas phase**

10

11           The measured mixing ratios of some organics (acetylene, isoprene, sum of  
12           monoterpenes, and acetone) as well as inorganic trace gases ( $\text{CO}$ ,  $\text{NO}$ ,  $\text{NO}_2$ ,  $\text{O}_3$ ) and wind  
13           direction are presented in Figure 4. Anthropogenic long-lived species such as acetylene and  
14            $\text{CO}$  present similar temporal variations during the campaign. Indeed, we noticed a slow  
15           variation of these compounds with a rise at the beginning of the campaign that reaches a  
16           maximum on 21 July and a subsequent decrease. The maximum corresponds to a period when  
17           air masses came from areas with strong emissions of anthropogenic species (North of Italy).  
18           However, the rise observed the previous days did not correspond to specific air mass cluster.  
19           Furthermore, the levels of anthropogenic species are very low at the measurement site (below  
20           200 ppt for acetylene, also observed for other anthropogenic compounds: e.g. below 80, 120  
21           and 150 ppt for benzene, n-butane and toluene, respectively) highlighting the probable lack of  
22           local anthropogenic sources. These very low levels of anthropogenic species at the ground  
23           level (often close to the limit of detection) made their measurements very challenging during  
24           the campaign.

25

26           On the contrary, significant levels of primary biogenic compounds were observed and  
27           could reached up to 1.2 and 2.0 ppb for isoprene and the sum of monoterpenes, respectively  
28           (Figure 4). These compounds were locally emitted by the typical vegetation of the  
29           Mediterranean region (“maquis” shrub-land) surrounding the measurement site. The mixing  
30           ratios for these compounds present a clear diurnal cycle with the highest values coinciding  
31           with maxima of temperature and solar radiation. Two periods characterized by high mixing  
32           ratios of biogenic VOCs were observed (27-28 July and 02-04 August), which correspond to  
33           the warmest periods of the campaign.

33

34           Oxygenated VOCs such as acetone were also present at significant levels: up to 3.8  
34           ppb (Figure 4). This compound has primary and secondary sources, issued from oxidation of



1 both biogenic and anthropogenic VOCs (see discussion in section 4.2.3). Therefore, acetone  
2 levels increase both when anthropogenic VOC concentrations increase (first part of the  
3 campaign) and when intense biogenic emission are observed (27-28 July and 02-04 August).

4  $\text{NO}_x$  levels remained low ( $<0.5$  and  $<2.0$  ppb for  $\text{NO}$  and  $\text{NO}_2$ , respectively) during the  
5 whole campaign. This confirms the lack of local anthropogenic sources close to the  
6 measurement site. Levels of  $\text{O}_3$  were very variable (20-80 ppb) with the highest levels  
7 encountered during the last part of the campaign. This period corresponded to the warmest  
8 period with intense biogenic emissions but also to air masses originating from the north of  
9 Italy, an area characterized by intense anthropogenic emissions of ozone precursors.

10 Oxygenated VOCs (including primary and secondary OVOCs from anthropogenic and  
11 biogenic origins) largely dominate the speciation of the measured VOCs (78%-80%, see Fig.  
12 S5 in supplements). OVOCs are dominated by methanol, acetone and formic acid which  
13 represent 28%, 23% and 14% of total OVOCs respectively. The weak contribution of  
14 biogenic hydrocarbons to the total VOC composition (4-5%, see Fig. S5 in supplements) is  
15 due to the fact that these contributions are calculated on a 24-h basis and not only during  
16 daytime when their concentrations are more elevated.

17 Finally, Anthropogenic NMHCs represent only 15-18% of the measured VOCs (see  
18 Fig. S5 in supplements), which is consistent with the remote location of the site. This VOC  
19 family is dominated by ethane, propane and ethylene which represent 34%, 7% and 7% of  
20 total A-NMHCs respectively. However, it is worth noting that this apportionment is only  
21 valuable for the measured species. Indeed, the difference between measured OH reactivity  
22 (total sink of OH) and calculated one, using all measured compounds, reported for this  
23 campaign indicates that approximately  $56\pm 15\%$  ( $1\sigma$ , on average) of the measured OH  
24 reactivity was missing. The largest fraction of missing OH reactivity was observed between  
25 23/07 and 30/07, a period associated to the Marine-West and South clusters (Zannoni et al.,  
26 2016). Therefore, a large fraction of the VOCs composing the air masses reaching the site has  
27 not been measured yet.

28

#### 29 4.1.2. Aerosol phase

30

31 The chemical composition derived from Q-ACSM measurements is reported in Figure  
32 5a for the period of study (15/07-05/08) and shows a clear and permanent dominance of OM  
33 which represents 55% of the total mass of  $\text{NR-PM}_{10}$  on average (average of  $3.74\pm 1.80 \mu\text{g m}^{-3}$ ),  
34 followed by sulphate (27%,  $1.83\pm 1.06 \mu\text{g m}^{-3}$ ), ammonium (13%,  $0.90\pm 0.55 \mu\text{g m}^{-3}$ ), and



1 nitrate (5%,  $0.31 \pm 0.18 \mu\text{g m}^{-3}$ ). These values are in the range of the monthly mean  
2 concentrations for summer calculated with Q-ACSM data over the two years period  
3 measurements (June 2012–July 2014) performed at the measurement site (J. Sciare,  
4 unpublished data). OM concentrations are comparable to those observed by Sciare et al.  
5 (2008) in the Eastern Mediterranean for the month of July ( $[\text{OC}] = 2.18 \pm 0.65 \mu\text{g m}^{-3}$  and  
6 using an OM-to-OC ratio of 1.9; Sciare et al., 2003). The overall OA concentrations during  
7 the campaign vary within two orders of magnitude (ranging from 0.13 to  $9.77 \mu\text{g m}^{-3}$ ) with  
8 very short periods (one to four hours) characterized by very sharp drops (close to zero)  
9 associated to clouds passing at the station and subsequent uptake of fine aerosols into the  
10 cloud droplets.

11 The temporal variability of OC and WSOC are reported in Figure 5b and show very  
12 close patterns with, however, few periods with noticeable discrepancies (17/07; 28/07–30/07).  
13 There is a clear correlation between the two datasets ( $r^2=0.68$ ;  $N=229$ ) with slope of 0.58  
14 reflecting that more than half of OC is water-soluble. The correlation between OC (OCEC  
15 Sunset Field Instrument) and OM (Q-ACSM) shows a better agreement ( $r^2=0.86$ ;  $N=229$ )  
16 with a slope of 0.87 when using an OC-to-OM ratio of 1.9. This slope close to one reflects the  
17 general good agreement between both instruments measuring OC in  $\text{PM}_{2.5}$  and OM in  $\text{PM}_{10}$ ,  
18 respectively. A closer look at the OM/OC ratio derived from these two instruments (not  
19 shown) shows a slight but systematic diurnal variability with minimum values around 09:00  
20 LT and a constant rise in the course of the day with a maximum value at 21:00 LT.  
21 Interestingly, although the absolute OM/OC ratio calculated empirically from Q-ACSM mass  
22 spectra (Aiken et al., 2008) should be interpreted with caution (Crenn et al., 2015), its  
23 temporal variability shows exactly the same diurnal pattern of local photochemical oxidation  
24 of OA, thus providing further consistency of our Q-ACSM fragmentation data which will be  
25 used later in the source apportionment.

26 Real-time observations of two light organic tracers (MSA and oxalate) are reported in  
27 Figure 5c. MSA (methanesulfonic acid,  $\text{CH}_3\text{SO}_3\text{H}$ ) is an oxidation end-product of  
28 dimethylsulfide (DMS), a natural gas produced from the marine phytoplankton activity. MSA  
29 is mostly in the aerosol phase and formed through the heterogeneous oxidation of  
30 dimethylsulfoxide (DMSO). It has been recently used to infer a marine organic aerosol (MOA)  
31 source from a source apportionment study performed in the region of Paris (France) (Crippa  
32 et al., 2013b). Oxalic acid is the most abundant dicarboxylic acid in the troposphere  
33 (Kawamura et al., 1996). Its primary sources cannot solely explain its observed ambient  
34 concentrations (Huang and Yu, 2007), suggesting that secondary formation processes remain



1 significant (Warneck, 2003). Simulations of these compounds predict reactions through in-  
2 cloud processing (Carlton et al., 2007; Ervens et al., 2004, 2008; Fu et al., 2008; Lim et al.,  
3 2005; Myriokefalitakis et al., 2011; Sorooshian et al., 2006; Volkamer et al., 2007; Warneck,  
4 2003). Field measurements also brought evidence of heterogeneous chemistry in the  
5 formation of oxalic acid through different routes (Crahan et al., 2004; Sorooshian et al., 2006,  
6 2007). Consequently real-time observations of MSA and oxalate may be used here in our  
7 source apportionment study to infer secondary oxidation processes.

8

## 9 **4.2 Exploring the drivers of VOC variability at Cape Corsica**

10

11 Source-receptor models, such as PMF, usually aim at identifying and quantifying the  
12 contributions of sources of pollutants impacting a measurement site. In our case, the remote  
13 location of the site combined with the reactivity of the selected species does not allow a  
14 proper identification and quantification of primary sources. Our main objective, here, lies  
15 within the identification of co-variation factors of species which could be representative of  
16 aged or fresh primary emission but also of photochemical processes occurring during long  
17 range transport or occurring locally. For this purpose, PMF was applied to a large dataset (42  
18 different species) including primary VOCs from anthropogenic or biogenic origins but also  
19 secondary products measured by three different techniques (PTR-ToF-MS, GC/FID-FID and  
20 GC/FID-MS, see section 2.2).

21 Figure 6 shows the time series of the 6 factors obtained by the PMF analysis. Figure 7  
22 shows the contributions of each factors to the species selected as inputs for the PMF model (in  
23 %) as well as the absolute averaged contribution of each species to the 6 factors determined  
24 by the PMF analysis (in ppt). Finally, Figure 8 presents the maps of simulated contributions  
25 (in ppt) using the CF model for 4 of the 6 PMF factors. The relative contributions of the  
26 different PMF factors to the sum of species used as inputs are presented in the Supplementary  
27 Material as Fig. S6.

28

### 29 **4.2.1 Anthropogenic influence**

30

31 Among the 6 PMF factors, three different factors were attributed to primary  
32 anthropogenic sources (Factors 2, 3, and 5) and are characterized by compounds of various  
33 lifetimes (Figure 6 & Figure 7). The lifetimes reported below are estimated from kinetic rate



1 constants of the reactions between the species of interest and OH, assuming an averaged OH  
2 concentration of  $2.0 \times 10^6$  molecules  $\text{cm}^{-3}$ .

3 Factor 2 is composed of long-lived primary anthropogenic species such as ethane  
4 (58% explained by Factor 2), acetylene (44% explained), propane (30% explained) and  
5 benzene (45% explained) (see Figure 7) with lifetimes ranging from 5 to 25 days and typically  
6 emitted by natural gas use and combustion processes. In addition to these long-lived primary  
7 anthropogenic species, other anthropogenic NMHCs, with shorter lifetimes, compose this  
8 factor, such as ethylene (35% explained) or 2-methyl-2-butene co-eluted with 1-pentene (42%  
9 explained). It tends to indicate that in addition of the lifetime, the nature of the sources (e.g.  
10 combustion processes) also partly influences the profile of this factor. Furthermore, Factor 2  
11 exhibits a behaviour similar to CO (see supplementary material S7), a long-lived compound  
12 (lifetime of ~24 days) mainly emitted by combustion processes, supporting the identification  
13 of this factor as long-lived anthropogenic. Hence, the lack of diurnal variability in this factor  
14 (see supplementary material S8) confirmed its long-range origin. The potential source areas  
15 associated with this factor (Figure 8) are the North of Italy (Po Valley) and the South East of  
16 France as well as, to a lower extent, the North-east of Tunisia (area of Tunis). These areas,  
17 and particularly the Po valley, are known to supply high anthropogenic emissions due to  
18 intense industrial activities and a dense road network (Thunis et al., 2009). This result  
19 strengthens the assumption of primary anthropogenic origin for this factor. This factor  
20 represents 16-17% of the sum of VOC species used as inputs in the PMF model  
21 (supplementary material Fig. S6).

22 Factor 3 is composed by medium-lived primary anthropogenic species such as n-  
23 pentane (78% explained by factor 3), iso-pentane (68% explained), 2,2dimethylbutane (48%  
24 explained) (see Figure 7) with lifetimes ranging from 1 to 3 days and typically emitted by  
25 gasoline evaporation or vehicle exhaust. This factor shows higher levels for air masses  
26 coming from the Europe-North-East and the France-North-West sectors (see Figure 6).  
27 Consequently, north of Italy (Po valley) and south-east of France, areas experiencing high  
28 anthropogenic emissions, are also identified as potential source areas for this factor (Figure 8).  
29 Potential source areas identified in the centre of France are most likely falsely attributed to  
30 this area due to corridor effect: the air masses reaching Cape Corsica and passing over the  
31 centre of France encompass systematically source areas (south-east of France). This factor  
32 represents 12% of the sum of VOC species used as inputs in PMF model (supplementary  
33 material Fig. S6).



1 Factor 5 is composed by short-lived primary anthropogenic VOCs such as ethylene  
2 (38% explained by factor 5), propene (44% explained) and toluene (38% explained) with  
3 lifetimes ranging from 5 to 23 h and typically emitted by combustion processes. This factor  
4 exhibits higher levels for air masses coming from the Corsica-South sector (see Figure 6).  
5 Likewise, areas at the south of Corsica are identified as potential source areas for this factor  
6 (Figure 8). Emissions of these areas could be due to both intense ship emissions, which  
7 speciation is dominated by alkenes (ethene, propene), aromatics and heavy alkanes ( $>C_6$ )  
8 (Eyring et al., 2005). A contribution of the Corsican cities in this southern sector cannot be  
9 excluded. This factor represents 21-23% of the sum of species used as inputs in the PMF  
10 model (supplementary material Fig. S6).

11 The total contribution of anthropogenic-like factors to the sum of species used as  
12 inputs of the PMF model is in the range 49-52%. This is higher than the contributions of  
13 anthropogenic NMHCs relatively to measured VOCs (15%, see Figure S5 in supplement).  
14 This can be explained by the fact that not only anthropogenic NMHCs contribute to these  
15 anthropogenic factors and some OVOCs are also part of them. For example, methanol and  
16 acetone contribute both in a non-negligible extent to these anthropogenic factors. Indeed,  
17 methanol contributes to 7% and 39% of LL-Anthropogenic factor and ML-Anthropogenic  
18 factor respectively; and acetone contributes to 14% and 11% of LL-Anthropogenic factor and  
19 SL-Anthropogenic factor respectively. Therefore, higher contributions of these factors to the  
20 gas phase composition are expected. Considering the primary anthropogenic part of OVOCs,  
21 determined based on the anthropogenic factor contribution to OVOCs, the contribution of  
22 anthropogenic VOCs to measured VOCs rises to 42% (see Figure 9), much closer to the PMF  
23 results.

24

#### 25 4.2.2 Biogenic influence

26

27 Among the 6 factors, two biogenic factors are also clearly identified (Factors 1 and 6).  
28 They are composed respectively by primary biogenic species (Factor 1) and oxidation  
29 products of primary biogenic hydrocarbons (Factor 6). Therefore, they have been classified  
30 and will be reported in the following respectively as “primary biogenic factor” (Factor 1) and  
31 “secondary biogenic factor” (Factor 6).

32 Indeed, Factor 1 is composed by primary biogenic species with very short lifetimes,  
33 emitted locally by the vegetation surrounding the measurement site, such as isoprene (68%  
34 explained by Factor 1), the sum of monoterpenes (83% explained) or camphor co-eluted with



1 undecane (38% explained) (see Figure 7). This factor exhibits clear diurnal cycles (Figure 6  
2 and supplementary material Fig. S8) and is correlated, as expected, with temperature (see  
3 supplementary material S7), which is well-known to influence biogenic emissions (Guenther  
4 et al., 1995; 2000).

5 This factor represents 14% of the sum of species used as inputs in the PMF model  
6 (supplementary material Fig. S6). This is higher than the contributions of biogenic NMHCs to  
7 measured VOCs (4-5%, see Fig. S5 in supplement). As already proposed for anthropogenic  
8 factors, this can be explained by the fact that not only biogenic NMHCs contribute to these  
9 primary biogenic factors but some biogenic OVOCs can also be part of it. For example,  
10 carboxylic acids, methanol and acetone also contribute (13%, 15% and 11% on average,  
11 respectively explained by factor 1). Taking into account the primary biogenic part of OVOCs,  
12 the contribution of biogenic VOCs to measured VOCs rises to 15% (see Figure 9), which is  
13 closer to the PMF results.

14 Factor 6 is composed by oxidation products of primary biogenic VOCs such as  
15 Methyl-Vinyl-Ketone (MVK) and methacrolein (MACR) (67% explained by Factor 6), which  
16 are measured as a sum by PTR-ToFMS ( $m/z$  71.05), nopinone (45% explained), and  
17 pinonaldehyde (39% explained) (see Figure 7). More specifically, MVK and MACR are first-  
18 generation oxidation products of isoprene (Miyoshi et al., 1994), nopinone is a first-  
19 generation oxidation product of  $\beta$ -pinene (Wisthaler et al., 2001), and pinonaldehyde is a first-  
20 generation oxidation product of  $\alpha$ -pinene (Wisthaler et al., 2001). As expected, the variability  
21 of this factor is also correlated to the temperature (see supplementary material S7). It can be  
22 explained by higher emissions of primary biogenic VOCs under warmer conditions associated  
23 with more intense photochemistry. Furthermore, the lowest levels of Factor 6 correspond to  
24 the highest wind speed observed at the measurement site and vice-versa (see Figure 6); near  
25 zero contributions of Factor 6 are observed on 23, 24 and 25 July when wind speeds were  
26 comprised between 3 and 10  $\text{m s}^{-1}$ . In contrast, the highest diurnal maxima were observed on  
27 26, 27 and 28 July and on 02 and 03 August when wind speeds did not exceed 3  $\text{m s}^{-1}$ . This  
28 factor is characterized by first-generation oxidation products of primary biogenic VOCs  
29 emitted in the vicinity of the site, and low wind speeds are necessary to observe them at  
30 significant levels. In case of high wind speed, these oxidation products undergo fast transport  
31 and dilution and low levels might be observed. This factor represents 6% of the sum of  
32 species used as inputs in the PMF model (supplementary material Fig. S6) and is therefore the  
33 less important.

34



### 1 4.2.3 Oxygenated Factor

2

3 The last factor (Factor 4) has been interpreted as “oxygenated factor” since it is mainly  
4 characterized by OVOCs such as carboxylic acids (54% formic acid, 43% acetic acid, 28%  
5 propionic acid, and 14% butyric acid), alcohols (49% methanol and 21% isopropanol),  
6 carbonyls (57% acetone, 18% acetaldehyde, and 21% methyl-ethyl-ketone). Most of these  
7 species are formed by the oxidation of both anthropogenic and biogenic compounds although  
8 some of them can also be directly emitted in the atmosphere and therefore can be of both  
9 primary and secondary origins. For example, methanol (the highest contributor to Factor 4)  
10 can be emitted by vegetation (MacDonald and Fall, 1993), biomass burning (Holzinger et al.,  
11 1999) or urban and industrial activities (Hu et al., 2011). It can also be formed by  
12 photochemistry (mainly photo-oxidation of methane) (Tyndall et al., 2001). The same stands  
13 for acetone (the 2<sup>nd</sup> highest contributor to Factor 4). Indeed, acetone can be directly emitted  
14 from vegetation (Goldstein and Schade, 2000; Hu et al., 2013), biomass burning (Simpson et  
15 al., 2011), and anthropogenic sources (Hu et al., 2013), and it can also be formed via  
16 photochemical oxidation of anthropogenic VOCs such as alkanes (Goldstein and Schade,  
17 2000) and biogenic VOCs such as monoterpenes (Reissell et al., 1999). Note that the same  
18 stands for carboxylic acids which also have multiple sources (de Angelis et al., 2012 and  
19 references therein).

20 The multi-sources pattern for this factor is highlighted by its time series. Indeed,  
21 Factor 4 exhibits a similar behaviour than anthropogenic factors (Factors 2 and 3) at the  
22 beginning of the campaign with an increase to reach a maximum around the 21 July and then  
23 a decrease. This Factor rises again during the intense biogenic influenced warm period (26, 27  
24 and 28 July) as observed for the secondary biogenic factor (Factor 6).

25 The CF analysis for this factor leads to the identification of the north of Italy and a  
26 large area in the southern of Corsica as potential source regions. North of Italy may contribute  
27 to the anthropogenic/continental influence of this factor while the large regions at the south of  
28 Corsica may contribute to the biogenic influence since the highest biogenic signature also  
29 corresponds to air masses coming from the Corsica-South sector. This could be explained by  
30 both potential biogenic emissions from vegetation of Corsica (the site being at the extreme  
31 north of the island) and/or warmer and more stagnant conditions arising when air masses  
32 came from Corsica-South sector favouring local biogenic emissions and low dispersion of  
33 oxidation products. It can also be due to local anthropogenic emissions from Corsica cities



1 erroneously attributed to more distant regions as already observed for the CF analysis of  
2 Factor 5. Finally, one cannot rule out the possibility of a primary or secondary influence of  
3 ship emissions to Factor 4 for this potential source area. This is also in accordance with the  
4 non-negligible contribution of this factor to the acetylene variability (29% explained by this  
5 factor). This factor represents 28-31% of the sum of species used as inputs in the PMF model  
6 (supplementary material Fig. S6) and is therefore the most important one. Combined with the  
7 secondary biogenic factor it leads to a contribution of 34-37% for the oxygenated factors. This  
8 is significantly lower than the OVOC contribution to the actual measured VOCs (80%, see  
9 Fig. S5) and can be explained by the contribution of most OVOCs such as acetone, methanol  
10 or carboxylic acids to other PMF factors. Only considering the secondary part of measured  
11 OVOCs, their contribution to measured VOCs decreases to 42% (see Figure 9), which is  
12 closer to the PMF results.

13

#### 14 **4.2.4 Apportionment of measured OVOC**

15

16 From the 6 PMF factors, it is possible to apportion the measured OVOCs among their  
17 potential different origins (primary anthropogenic or biogenic emissions, photochemical  
18 production from the oxidation of anthropogenic or biogenic hydrocarbons). Therefore, Factor  
19 1 is attributed to a primary biogenic origin, Factors 2, 3 and 5 are attributed to a primary  
20 anthropogenic origin and factors 4 and 6 are attributed to a secondary origin (photochemical  
21 oxidation of primary VOCs from both biogenic and anthropogenic origins). To do so, the  
22 contributions of each OVOC to a specific PMF factor are summed up and ascribed to the  
23 corresponding origin. Subtracted backgrounds of acetone and methanol are redistributed to  
24 each PMF factors accordingly to the relative contribution of these species to each factor. The  
25 apportionment of anthropogenic, biogenic and secondary origin for OVOCs can be seen in  
26 Figure 9. Primary anthropogenic sources, primary biogenic sources and secondary processes  
27 account for 34%, 13% and 53% of the measured OVOCs, respectively. Therefore, measured  
28 OVOCs at cape Corsica are approximately half oxidation products of VOCs and half primary  
29 VOCs.

30

#### 31 **4.2.5 Comparison with other PMF studies performed in remote environments**

32

33 To our best knowledge, only three studies have been conducted applying PMF for gas  
34 phase species in remote environments (Sauvage et al., 2009; Lanz et al., 2009; Leuchner et al.,



1 2015). Moreover, these studies were only based on NMHC measurements, and chlorinated  
2 organic species for one of them (Lanz et al., 2009). No oxygenated VOCs were considered.  
3 Consequently, these three studies only identified factors representative of primary sources.

4 Indeed, Leuchner et al. (2015) identified 6 PMF factors, at a remote site at  
5 Hohenpeissenberg over a period of 7 years (2003-2009), including primary biogenic, short-  
6 lived combustion, short-lived evaporative, residential heating, long-lived evaporative and  
7 background factors. Therefore, the classification of factors was linked to the difference in the  
8 sources typology (biogenic vs anthropogenic, combustion vs evaporative) and/or the lifetime  
9 of compounds (short-lived vs long-lived). Lanz et al. (2009) found only 4 PMF factors, at a  
10 continental mountain site at Jungfrauoch (Switzerland) during height years (2000-2007),  
11 including a highly aged combustive emissions factor correlated to CO, a fresh emissions and  
12 solvent-use factor correlated to NO<sub>x</sub>, and two industrial factors mainly explaining the  
13 variability of chlorinated compounds. Sauvage et al. (2009) applied PMF to a database of  
14 NMHCs measured at three background sites in France, leading to 5 common PMF factors  
15 including evaporative sources, residential heating, vehicle exhaust, remote sources attributed  
16 to aged background air and biogenic emissions.

17 Therefore, we incorporated for the first time OVOCs in a database used for PMF  
18 analysis at a remote environment. It allows the first identification of PMF factors  
19 representatives of secondary processes in addition to factors related to primary sources. As it  
20 has been found in previous studies performed in such environments, we also found that  
21 primary anthropogenic PMF factors were separated according to the lifetime of compounds  
22 which composed them. As in the three studies described above, a clear primary biogenic  
23 factor is identified in our study. Furthermore, our analysis allowed the apportionment of the  
24 anthropogenic, biogenic and secondary parts of OVOCs.

25

### 26 **4.3 Source apportionment of OA at cape Corsica**

27

28 Based on the two available months of ACSM data, a 3-factor solution was selected  
29 here, corresponding to a minimum of the quality parameter Q/Q<sub>exp</sub>. Mass spectra reported in  
30 Figure 10 show a typical HOA (Hydrogen-like OA) profile for the first factor with n-alkanes,  
31 branched alkanes, cycloalkanes, and aromatics, leading to high signals at the ion series  
32 C<sub>n</sub>H<sup>+</sup><sub>2n+1</sub> and C<sub>n</sub>H<sup>+</sup><sub>2n-1</sub> (m/z 27, 29, 41, 43, 55, 57, 69, 71, etc.) and typical for fossil fuel  
33 combustion (Canagaratna et al., 2004; Chirico et al., 2010). We have also used the terms “SV-  
34 OOA” (Semi-Volatile-Oxygenated Organic Aerosol) and “LV-OOA” (Low-Volatile OOA) as



1 introduced by Jimenez et al. (2009) to describe the two remaining factors. In these two  
2 factors,  $m/z$  43 and  $m/z$  44 are the most prominent peaks which is consistent with OOA  
3 (Oxygenated OA) spectra and the  $m/z$  44 to  $m/z$  43 ratio that increases with aging (Ng et al.,  
4 2010a). The signal at  $m/z$  43 is dominant for the second factor and mainly comes from the  
5 fragmentation of either hydrocarbon chains to form  $C_3H_7^+$  or carbonyls to form  $C_2H_3O^+$ ;  
6 therefore this factor appears to be the less oxidized and was named consequently SV-OOA.

7 The consistency of the different OA factors was further checked with external tracers  
8 in Figure 11; HOA with BC (fossil fuel tracer), SV-OOA with WSOC, and LV-OOA with  
9 oxalate. The good agreement of SV-OOA with WSOC is consistent with freshly formed SOA  
10 being semi-volatile and water-soluble as reported for instance by Hennigan et al. (2008a) who  
11 observed strong similarities between semi-volatile  $NH_4NO_3$  and (PILS-TOC based) WSOC.  
12 The good agreement between LV-OOA with oxalate is consistent with the fact that both are  
13 mostly composed by carboxylic acid COO chains and the use of oxalate as a proxy of highly  
14 oxidized OA as stated before. Note also that good correlation is obtained between the  
15 averaged OOA mass spectra taken from Ng et al. (2010b) and our two factors with correlation  
16 coefficients ( $r^2$ ) of 0.96 and 0.81 for our SV-OOA and LV-OOA factors, respectively.

17 The different OA factors obtained here are mainly of continental origin and therefore,  
18 their temporal variability is mostly related to the amount and frequency of continental air  
19 masses reaching the sampling site. Nevertheless, the diurnal variation of SV-OOA and LV-  
20 OOA (Fig S9) suggest that local photochemical processes have also occurred, with local  
21 formation of fresh SV-OOA in the morning followed by a rapid oxidation which could  
22 explain the enhancement of LV-OAA in the afternoon.

23 Average mass concentrations are 0.13, 1.59, and  $1.92 \mu\text{g m}^{-3}$  for the 3 determined  
24 factors HOA, SV-OOA, and LV-OOA, respectively, for a total average OA concentration of  
25  $3.63 \mu\text{g m}^{-3}$  and a contribution of OA to NR- $PM_{10}$  of 52%. As a result, secondary OA  
26 represent about 96% of OA with aged (LV-)OOA contributing for approximately 55% of this  
27 secondary OA fraction. In the recent years, increasing background OA observations have  
28 become available in the Mediterranean, mostly at coastal sites located in the Northern part of  
29 the basin (Spain, France, Italy, and Greece). For instance, long-term (13-months) ACSM  
30 measurements were performed at a regional background site in the western Mediterranean  
31 (Spain), located in the Montseny natural park 50 km North-North-East of Barcelona,  
32 approximately 500 km west of Cape Corsica, and reported observations similar to ours with  
33 an OA contribution to NR- $PM_{10}$  of c.a. 60% (Minguillon et al., 2015), three major OA sources



1 (HOA, SV-OOA, and LV-OOA) during summer with again a very prominent secondary  
2 fraction (85% of OA), and OA profiles very similar to those obtained here.

3

#### 4 **4.4 Gas-aerosol link**

5

6 First, the gas-phase “Oxygenated Factor” (Factor 4) is correlated to the organic  
7 fraction of the aerosol measured by ACSM ( $R^2=0.58$ ,  $n=498$ ; see supplementary material S7).  
8 This fair correlation likely highlights the close link between gaseous oxidation products  
9 observed at the site and measured Organic Aerosol (OA) since they stem from similar  
10 processes. During the campaign, very low levels of Primary Organic Aerosols were observed  
11 (HOA determined by ACSM measurements below  $0.4 \mu\text{g m}^{-3}$ , see Figure 11a (top panel)).  
12 Thus, this correlation is most likely due to the secondary fraction of OA, representing 96% of  
13 OA (see section 4.3), which can come from the oxidation of both biogenic and anthropogenic  
14 gaseous precursors, explaining the similar behaviour as Factor 4.

15 Figure 12 shows stacked time series of the different fractions (inorganic and organic)  
16 of aerosol measured by ACSM (top panel) as well as stacked time series of contributions of  
17 PMF factors (middle panel) for the VOCs (see section 4.2). This figure aims at drawing a  
18 parallel between aerosol and gas phase compositions to highlight the link between the two  
19 phases.

20 From these graphs and from the back-trajectory clusters (also shown in Figure 12), it  
21 is possible to distinguish two periods during which processed anthropogenic/continental air  
22 masses reached the site (between 19 and 27 July and between 30 July and 03 August 2013).  
23 The first period is characterized by high contributions of anthropogenic and oxygenated gas  
24 PMF factors (middle panel of Figure 12) as well as an aerosol with inorganic (ammonium  
25 sulphate) and organic fractions in approximately similar proportions (top panel of Figure 12).  
26 This period also corresponds to the highest values of  $\ln(\text{propane/ethane})$  ( $-1.4$  on average and  
27 up to  $-0.8$ , see bottom panel of Figure 12) hence the less aged air masses, coinciding with the  
28 Europe-North-East sector. The second period of long-range transported  
29 anthropogenic/continental emissions is characterized by less intense anthropogenic gas phase  
30 PMF factors, especially for the long-lived anthropogenic factor, and a clear predominance of  
31 the organic fraction for aerosols. Aerosol mass concentrations are also lower by  
32 approximately 50% compared to the first period. During both periods, a non-negligible  
33 biogenic influence is also observed from primary and secondary biogenic PMF VOC factors.  
34 This is even more pronounced for the second “anthropogenic” period. During these periods it



1 is, therefore, likely that oxygenated VOCs and OOA have both biogenic and anthropogenic  
2 origins in variable proportions.

3 A period of intense biogenic influence, without significant long-range transport of  
4 anthropogenic/continental emissions, can also be distinguished (between 26 and 28 July) with  
5 elevated contributions of the primary and secondary biogenic gas-phase PMF factors (Figure  
6 12). The oxygenated gas-phase PMF factor also rose during this period and the aerosol  
7 composition is dominated by OA with low levels of inorganic aerosols. Indeed, the inorganic  
8 fraction of aerosols decreases to reach less than 10% of the aerosol composition on 27 July.  
9 This strong decrease occurred at the same time than a change of air mass origin from Marine-  
10 West to Corsica-South. This is consistent with the lack of anthropogenic influence during this  
11 period, confirmed by lower  $\ln(\text{propane/ethane})$  (-1.8 on average up to -2.3, see bottom panel  
12 of Figure 12). It is, therefore, likely that the oxygenated VOCs and the organic fraction of  
13 aerosols during these days are mainly influenced by biogenic sources.

14 Finally, very low contributions of HOA were observed during the whole campaign  
15 from the PMF analysis of ACSM measurements (typically below  $0.3 \mu\text{g m}^{-3}$  all along the  
16 campaign). This illustrates the weak influence of freshly emitted primary anthropogenic  
17 sources of OA at the site. This is also confirmed by low levels of black carbon ( $\text{BC} < 0.9 \mu\text{g m}^{-3}$   
18 for the whole campaign, see Figure 11a).

19 An analysis of the isotopic ratio of  $^{14}\text{C}$  in aerosol sampled at cape Corsica reveals that  
20 the organic fraction of the aerosol measured during the ChArMEx SOP2 field campaign  
21 mainly came from biogenic sources and the oxidation of biogenic VOCs with measured non-  
22 fossil OC of  $2.42 \pm 0.86 \mu\text{gC m}^{-3}$  on average (76 $\pm$ 3 % of OC on average). The secondary and  
23 primary anthropogenic sources to OC represented by measured fossil OC was  
24  $0.44 \pm 0.22 \mu\text{gC m}^{-3}$  on average with a contribution to OC being 14 $\pm$ 3 % of OC on average.  
25 Elementary carbon contributed to only 10% of total carbon during the campaign with  
26 averaged measure biomass EC and fossil EC being  $0.16 \pm 0.06 \mu\text{gC m}^{-3}$  and  $0.17 \pm 0.06 \mu\text{gC m}^{-3}$   
27 respectively. Results from this analysis will be presented in more details in a forthcoming  
28 paper (Pey et al., in preparation).

29 Given the good correlation observed between OA and the gas-phase oxygenated factor  
30 ( $R^2=0.58$ ,  $n=498$ ), a common origin can be attributed to both OA and OVOCs observed at  
31 Cape Corsica. Therefore, a predominance of secondary biogenic origin, during the whole  
32 campaign, is likely for OVOCs, such as acetone, methanol or carboxylic acids for example,  
33 which composed the oxygenated PMF factor. As stated previously, this is also consistent with  
34 the large fraction of WSOC in OA, whose fraction usually refers to biogenic SOA.



1 Nevertheless, a less important but still significant secondary anthropogenic origin is also  
2 likely for OVOCs.

3

## 4 **5 Conclusions**

5

6 The ChArMEx SOP2 field campaign provided a unique opportunity to give insights in  
7 the various sources and fates of organic carbon in the Mediterranean atmosphere, thanks to  
8 the measurement of a large panel of gaseous and aerosol species at a remote site located at  
9 Cape Corsica in the western Mediterranean basin. The combination of gaseous and particulate  
10 organic databases, as collected during this campaign, is not common and has the potential to  
11 help improving our understanding of SOA formation. Moreover, the Mediterranean basin is  
12 an ideal location to characterize organics in the atmosphere since it is impacted by strong  
13 natural and anthropogenic sources and undergoes intense photochemical ageing especially  
14 during summer. The measurement site (Cape Corsica) offered ideal experimental conditions  
15 since it is surrounded by the sea and it is located at various distances from regional  
16 anthropogenic emissions hotspots (such as north of Italy, south-east of France, north-east of  
17 Spain or north of Africa). These characteristics coupled to extremely low local anthropogenic  
18 sources allowed the study of anthropogenic plumes after several days of atmospheric  
19 processing. In addition, intense local biogenic emissions permitted the investigation of  
20 biogenic and anthropogenic interactions on air mass composition.

21 These specific conditions led to the observation of contrasted situations, i.e. highly  
22 variable photochemical ages of processed anthropogenic air masses coupled with intense and  
23 local biogenic emissions. Low levels of anthropogenic VOCs (<250 ppt for acetylene for  
24 example) were overall observed, confirming the remoteness of the site. In contrast, significant  
25 levels of short-lived biogenic VOCs (up to 1.2 and 2.0 ppb for isoprene and the sum of  
26 monoterpenes, respectively) were observed. Elevated mixing ratios of OVOCs (e.g. up to 3.8  
27 ppb for acetone) were also measured during the campaign due to the oxidation of both  
28 biogenic and anthropogenic precursors. These OVOCs exhibit the largest contribution to the  
29 VOC budget.

30 The aerosol chemical composition derived from Q-ACSM measurements shows a  
31 clear predominance of OM, which represents 55% of the total mass of NR-PM<sub>1</sub> on average,  
32 followed by sulphate (27%), ammonium (13%), and nitrate (5%). Furthermore, the temporal  
33 variability of OC and WSOC shows very similar patterns, leading to a clear linear correlation



1 between the two datasets ( $r^2=0.68$ ). The slope found is 0.58, highlighting that more than half  
2 of OC is water-soluble.

3 PMF was conducted to identify co-variation factors of VOCs that are representative of  
4 primary emissions as well as secondary photochemical transformations occurring during the  
5 transport of air masses. This analysis was performed using a gas-phase database of 42 VOCs  
6 (or sum of VOCs) of anthropogenic and biogenic origins, including NMHCs and for the first  
7 time OVOCs. A 6-factor solution turned out to be optimum for this PMF analysis. In parallel,  
8 a concentration field (CF) analysis was conducted on 4 PMF factor to help in their  
9 identification through the localization of potential source areas. This combination of CF and  
10 PMF was particularly helpful to interpret factors associated to long-range transport of  
11 anthropogenic compounds.

12 Three anthropogenic factors characterized by primary anthropogenic VOCs of various  
13 lifetimes were found. The CF analysis confirmed the anthropogenic nature of these factors by  
14 an identification of potential source areas in region experiencing intense anthropogenic  
15 activities (e.g. Po valley and south-east of France).

16 Two biogenic factors were also identified. Both factors exhibited clear diurnal cycles  
17 and were correlated to temperature. In addition to a primary biogenic factor, usually observed  
18 in VOC source apportionment studies, we also clearly identified, for the first time in PMF  
19 analysis, a secondary biogenic factor made of first-generation oxidation products of biogenic  
20 VOCs.

21 A last oxygenated factor characterized by OVOCs of both biogenic and anthropogenic  
22 origins, was also derived from the PMF analysis. The identification of this unusual factor was  
23 made possible by the extension of the input database to secondary oxygenated VOCs. This  
24 factor was influenced by anthropogenic and biogenic sources showing elevated levels during  
25 both periods of intense local biogenic influence (e.g. 26-28 July) and periods of long-range  
26 transport of anthropogenic/continental emissions (e.g. 21-23 July). This factor was also  
27 correlated to submicron OA measured by ACSM ( $R^2=0.58$ ,  $n=498$ ), highlighting the close  
28 link between secondary OVOCs and (secondary) OA at cape Corsica. The CF analysis of this  
29 factor suggested potential source areas that could be attributed to both  
30 anthropogenic/continental (North of Italy) and biogenic influences (areas at the south of  
31 Corsica).

32 The source apportionment of OA measured by ACSM led to a 3-factor solution  
33 identified as hydrogen-like OA, semi-volatile oxygenated OA, and low-volatile oxygenated  
34 OA. These 3 factors accounted for an averaged mass concentration of 0.13, 1.59, and 1.92  $\mu\text{g}$



1  $\text{m}^{-3}$ , respectively, for a total OA mass concentration of  $3.63 \mu\text{g m}^{-3}$ , mainly associated to  
2 secondary formation (96%).

3 A coupled analysis of VOC and OA sources was conducted. During biogenic periods,  
4 the aerosol composition was dominated by (secondary) OA, while during periods of long-  
5 range transport of anthropogenic/continental emissions, the inorganic and organic fractions of  
6 submicron aerosol were similar. During the whole campaign, low levels of Hydrogen-like OA  
7 (HOA) were observed ( $<0.3 \mu\text{g m}^{-3}$ ), indicating a weak influence of primary anthropogenic  
8 sources on OA. Finally, the analysis of the isotopic ratio of  $^{14}\text{C}$  in  $\text{PM}_{10}$ , which will be  
9 presented in detail in a forthcoming paper, highlighted that OA aerosols were mainly  
10 produced from the local oxidation of biogenic VOCs. Given the good correlation between the  
11 oxygenated gas phase PMF factor and organic aerosols, the same origin is likely for OVOCs  
12 with a predominance of sources from the oxidation of BVOCs.

13

#### 14 **Acknowledgements**

15

16 This study received financial support from Mistrals / ChArMEx programmes,  
17 ADEME, the French environmental ministry, the CaPPA projects and the Communauté  
18 Territoriale de Corse (CORSiCA project). The CaPPA project (Chemical and Physical  
19 Properties of the Atmosphere) is funded by the French National Research Agency (ANR)  
20 through the PIA (Programme d'Investissement d'Avenir) under contract "ANR-11-LABX-  
21 0005-01" and by the Regional Council Nord-Pas de Calais and the "European Funds for  
22 Regional Economic Development" (FEDER). This research was also funded by the European  
23 Union Seventh Framework Programme under Grant Agreement number 293897, "DEFIVOC"  
24 project, CARBOSOR/Primequal and SAF-MED (ANR, grant number: ANR-12-BS06-0013-  
25 02). Greenhouse gases data were provided by the ICOS-France monitoring network.

26 The authors also want to thank Eric Hamonou and François Dulac for logistic help  
27 during the campaign as well as all the participants of the ChArMEx SOP2 field campaign.



## 1 References

- 2 ACTRIS Measurement Guidelines VOC, WP4-NA4: Trace gases networking: Volatile  
3 organic carbon and nitrogen oxides Deliverable D4.1: Draft for standardized operating  
4 procedures (SOPs) for VOC measurements, [http://ebas-](http://ebas-submit.nilu.no/Portals/117/media/SOPs/MG_VOC_draft_20120718.pdf)  
5 [submit.nilu.no/Portals/117/media/SOPs/MG\\_VOC\\_draft\\_20120718.pdf](http://ebas-submit.nilu.no/Portals/117/media/SOPs/MG_VOC_draft_20120718.pdf), p: 24-32, 2012
- 6 Aiken, A. C., DeCarlo, P. F., Kroll, J. H., Worsnop, D. R., Huffman, J. A., Docherty, K. S.,  
7 Ulbrich, I. M., Mohr, C., Kimmel, J. R., Sueper, D., Sun, Y., Zhang, Q., Trimborn, A.,  
8 Northway, M., Ziemann, P. J., Canagaratna, M. R., Onasch, T. B., Alfarra, M. R., Prevot, A.  
9 S. H., Dommen, J., Duplissy, J., Metzger, A., Baltensperger, U., and Jimenez, J. L.: O/C and  
10 OM/OC ratios of primary, secondary, and ambient organic aerosols with high-resolution time-  
11 of-flight aerosol mass spectrometry, *Environ. Sci. Technol.*, 42, 4478–4485, 2008.
- 12 Ait-Helal, W., Borbon, A., Sauvage, S., de Gouw, J. A., Colomb, A., Gros, V., Freutel, F.,  
13 Crippa, M., Afif, C., Baltensperger, U., Beekmann, M., Doussin, J.-F., Durand-Jolibois, R.,  
14 Fronval, I., Grand, N., Leonardis, T., Lopez, M., Michoud, V., Miet, K., Perrier, S.,  
15 Prévôt, A. S. H., Schneider, J., Siour, G., Zapf, P., and Locoge, N.: Volatile and intermediate  
16 volatility organic compounds in suburban Paris: variability, origin and importance for SOA  
17 formation, *Atmos. Chem. Phys.*, 14, 10439-10464, doi:10.5194/acp-14-10439-2014, 2014
- 18 Ashbaugh, L. L., Malm, W. C., and Sadeh, W. Z.: A residence time probability analysis of  
19 sulfur concentrations at grand-canyonnational-park, *Atmos. Environ.*, 19, 1263–1270, 1985.
- 20 Atkinson, R.: Atmospheric chemistry of VOCs and NO<sub>x</sub>, *Atmos. Environ.*, 34, 2063-2101,  
21 10.1016/s1352-2310(99)00460-4, 2000.
- 22 Aumont, B., Szopa, S., and Madronich, S.: Modelling the evolution of organic carbon during  
23 its gas-phase tropospheric oxidation: development of an explicit model based on a self  
24 generating approach, *Atmos. Chem. Phys.*, 5, 2497-2517, doi:10.5194/acp-5-2497-2005,  
25 2005.
- 26 Aumont, B., Valorso, R., Mouchel-Vallon, C., Camredon, M., Lee-Taylor, J., and Madronich,  
27 S.: Modeling SOA formation from the oxidation of intermediate volatility n-alkanes, *Atmos.*  
28 *Chem. Phys.*, 12, 7577–7589, doi: 10.5194/acp-12-7577-2012, 2012
- 29 Badol, C., Borbon, A., Locoge, N., Leonardis, T., Galloo, J.C.: An automated monitoring  
30 system for VOC ozone precursors in ambient air: development, implementation and data  
31 analysis. *Anal. Bioanal. Chem.*, 378, 7, 1815–1827, 2004
- 32 Bae, M.-S., Schauer, J. J., DeMinter, J. T., Turner, J. R., Smith, D., and Cary, R. A.:  
33 Validation of a semi-continuous instrument for elemental carbon and organic carbon using a  
34 thermal-optical method, *Atmos. Environ.* 38, 2885–2893, 2004.
- 35 Budisulistiorini, S. H., Baumann, K., Edgerton, E. S., Bairai, S. T., Mueller, S., Shaw, S. L.,  
36 Knipping, E. M., Gold, A., and Surratt, J. D.: Seasonal characterization of submicron aerosol  
37 chemical composition and organic aerosol sources in the southeastern United States: Atlanta,  
38 Georgia and Look Rock, Tennessee, *Atmos. Chem. Phys. Discuss.*, 15, 22379–22417, doi:  
39 10.5194/acpd-15-22379-2015, 2015.



- 1 Canagaratna, M. R., Jayne, J. T., Ghertner, D. A., Herndon, S., Shi, Q., Jimenez, J. L., Silva,  
2 P. J., Williams, P., Lanni, T., Drewnick, F., Demerjian, K. L., Kolb, C. E., and Worsnop, D.  
3 R.: Chase studies of particulate emissions from in-use New York City vehicles, *Aerosol Sci.*  
4 *Techn.*, 38, 555–573, 2004.
- 5 Canonaco, F., Crippa, M., Slowik, J. G., Baltensperger, U., and Prévôt, A. S. H.: SoFi, an  
6 IGOR-based interface for the efficient use of the generalized multilinear engine (ME-2) for  
7 the source apportionment: ME-2 application to aerosol mass spectrometer data, *Atmos. Meas.*  
8 *Techn.*, 6, 3649–3661, doi: 10.5194/amt-6-3649-2013, 2013.
- 9 Carlton, A. G., Turpin, B. J., Altieri, K. E., Seitzinger, S., Reff, A., Lim, H. J., and Ervens, B.,  
10 Atmospheric oxalic acid and SOA production from glyoxal: Results of aqueous  
11 photooxidation experiments, *Atmos. Environ.*, 41(35), 7588-7602, 2007
- 12 CCI Territorial Bastia Haute Corse: Port de Bastia Statistiques Portuaires 2013,  
13 [http://www.bastia-hautecorse.cci.fr/PortBia/images/stats/annuel\\_2014\\_bastia\\_2013.pdf](http://www.bastia-hautecorse.cci.fr/PortBia/images/stats/annuel_2014_bastia_2013.pdf), 2013
- 14 Charron, A., Plaisance, H., Sauvage, S., Coddeville, P., Galoo, J.C., Guillermo, R.: A study of  
15 the source-receptor relationships influencing the acidity of precipitation collected at a rural  
16 site in France. *Atmos. Environ.*, 34, 3665-3674, 2000
- 17 Chirico, R., DeCarlo, P. F., Heringa, M. F., Tritscher, T., Richter, R., Prévôt, A. S. H., and  
18 Laborde, M., Impact of aftertreatment devices on primary emissions and secondary organic  
19 aerosol formation potential from in-use diesel vehicles: results from smog chamber  
20 experiments, *Atmos. Chem. Phys.*, 10(23), 11545-11563, 2010
- 21 Crahan, K. K., Hegg, D., Covert, D. S., and Jonsson, H., An exploration of aqueous oxalic  
22 acid production in the coastal marine atmosphere, *Atmos. Environ.*, 38(23), 3757-3764, 2004
- 23 Crenn, V., Sciare, J., Croteau, P. L., Verlhac, S., Fröhlich, R., Belis, C. A., Aas, W., Äijälä,  
24 M., Alastuey, A., Artiñano, B., Baisnée, D., Bonnaire, N., Bressi, M., Canagaratna, M.,  
25 Canonaco, F., Carbone, C., Cavalli, F., Coz, E., Cubison, M. J., Esser-Gietl, J. K., Green, D.  
26 C., Gros, V., Heikkinen, L., Herrmann, H., Lunder, C., Minguillón, M. C., Močnik, G.,  
27 O'Dowd, C. D., Ovadnevaite, J., Petit, J.-E., Petralia, E., Poulain, L., Priestman, M., Riffault,  
28 V., Ripoll, A., Sarda-Estève, R., Slowik, J. G., Setyan, A., Wiedensohler, A., Baltensperger,  
29 U., Prévôt, A. S. H., Jayne, J. T., and Favez, O.: ACTRIS ACSM intercomparison – Part 1:  
30 Reproducibility of concentration and fragment results from 13 individual Quadrupole Aerosol  
31 Chemical Speciation Monitors (Q-ACSM) and consistency with co-located instruments,  
32 *Atmos. Meas. Techn.*, 8, 5063-5087, doi:10.5194/amt-8-5063-2015, 2015.
- 33 Crippa, M., Canonaco, F., Slowik, J. G., El Haddad, I., DeCarlo, P. F., Mohr, C., Heringa, M.  
34 F., Chirico, R., Marchand, N., Temime-Roussel, B., Abidi, E., Poulain, L., Wiedensohler, A.,  
35 Baltensperger, U., and Prévôt, A. S. H.: Primary and secondary organic aerosol origin by  
36 combined gas-particle phase source apportionment, *Atmos. Chem. Phys.*, 13, 8411–8426,  
37 doi:10.5194/acp-13-8411-2013, 2013a
- 38 Crippa, M., El Haddad, I., Slowik, J. G., DeCarlo, P. F., Mohr, C., Heringa, M. F., Chirico,  
39 R., Marchand, N., Sciare, J., Baltensperger, U., and Prévôt, A. S. H.: Identification of marine  
40 and continental aerosol sources in Paris using high resolution aerosol mass spectrometry, *J.*  
41 *Geophys. Res.-Atmos.*, 118, 1950–1963, 2013b.



- 1 de Angelis, M., Traversi, R., Udisti, R.: Long-term trends of mono-carboxylic acids in  
2 Antarctica: comparison of changes in sources and transport processes at the two EPICA deep  
3 drilling sites, *Tellus B*, 64, 17331, DOI: 10.3402/tellusb.v64i0.17331, 2012
- 4 de Gouw, J. and Warneke, C.: Measurements of volatile organic compounds in the earth's  
5 atmosphere using proton-transferreaction mass spectrometry, *Mass. Spectrom. Rev.*, 26, 223–  
6 257, doi:10.1002/mas.20119, 2007.
- 7 Detournay, A., Sauvage, S., Locoge, N., Gaudion, V., Leonardis, T., Fronval, I., Kaluzny, P.,  
8 and Galloo, J.-C.: Development of a sampling method for the simultaneous monitoring of  
9 straightchain alkanes, straight-chain saturated carbonyl compounds and monoterpenes in  
10 remote areas. *J. Environ. Monitor.*, 13, 983– 990, 2011.
- 11 Draxler, R. R. and Hess, G. D.: An overview of the HYSPLIT 4 modeling system for  
12 trajectories, dispersion, and deposition, *Aust. Meteorol. Mag.*, 47, 295–308, 1998.
- 13 Ervens, B., Feingold, G., Frost, G. J., and Kreidenweis, S. M., A modeling study of aqueous  
14 production of dicarboxylic acids: 1. Chemical pathways and speciated organic mass  
15 production, *J. Geophys. Res.-Atmos.*, 109(D15), 2004
- 16 Ervens, B., Carlton, A. G., Turpin, B. J., Altieri, K. E., Kreidenweis, S. M., and Feingold, G.,  
17 Secondary organic aerosol yields from cloud-processing of isoprene oxidation products,  
18 *Geophys. Res. Lett.*, 35(2), 2008
- 19 Eyring, V., Kohler, H. W., van Aardenne, J., and Lauer, A.: Emissions from international  
20 shipping: 1. The last 50 years, *J. Geophys. Res.*, 110, D17305, doi:10.1029/2004JD005619,  
21 2005.
- 22 Fares, S., Park, J. H., Gentner, D. R., Weber, R., Ormeno, E., Karlik, J., and Goldstein, A. H.:  
23 Seasonal cycles of biogenic volatile organic compound fluxes and concentrations in a  
24 California citrus orchard, *Atmos. Chem. Phys.*, 12, 9865–9880, doi:10.5194/acp- 12-9865-  
25 2012, 2012.
- 26 Forster, P., Ramaswamy, V., Artaxo, P., Berntsen, T., Betts, R., Fahey, D. W., Haywood, J.,  
27 Lean, J., Lowe, D. C., Myhre, G., Nganga, J., Prinn, R., Raga, G., Schulz, M., and Van  
28 Dorland, R.: Radiative Forcing of Climate Change, in: *Climate Change 2007: The Physical  
29 Science Basis, Contribution of Working Group I to the Fourth Assessment Report of the  
30 Intergovernmental Panel on Climate Change*, edited by: Solomon, S., Qin, D., Manning, M.,  
31 Chen, Z., Marquis, M., Averyt, K. B., Tignor, M., and Miller, H. L., 2007
- 32 Fröhlich, R., Crenn, V., Setyan, A., Belis, C. A., Canonaco, F., Favez, O., Riffault, V.,  
33 Slowik, J. G., Aas, W., Aijälä, M., Alastuey, A., Artiñano, B., Bonnaire, N., Bozzetti, C.,  
34 Bressi, M., Carbone, C., Coz, E., Croteau, P. L., Cubison, M. J., Essergietl, J. K., Green, D.  
35 C., Gros, V., Heikkinen, L., Herrmann, H., Jayne, J. T., Lunder, C. R., Minguillón, M. C.,  
36 Mocnik, G., O'Dowd, C. D., Ovadnevaite, J., Petralia, E., Poulain, L., Priestman, M., Ripoll,  
37 A., Sarda-Estève, R., Wiedensohler, A., Baltensperger, U., Sciare, J., and Prévôt, A. S. H.:  
38 ACTRIS ACSM intercomparison – Part 2: Intercomparison of ME-2 organic source  
39 apportionment results from 15 individual, co-located aerosol mass spectrometers, *Atmos.*  
40 *Meas. Tech.*, 8, 2555–2576, doi: 10.5194/amt-8-2555-2015, 2015.



- 1 Fu, T. M., Jacob, D. J., Wittrock, F., Burrows, J. P., Vrekoussis, M., and Henze, D. K., Global  
2 budgets of atmospheric glyoxal and methylglyoxal, and implications for formation of  
3 secondary organic aerosols, *J. Geophys. Res.-Atmos.*, 113(D15), 2008
- 4 Gaimoz, C., Sauvage, S., Gros, V., Herrmann, F., Williams, J., Locoge, N., Perrussel, O.,  
5 Bonsang, B., d'Argouges, O., SardaEsteve, R., and Sciare, J.: Volatile Organic Compounds  
6 sources in Paris in spring 2007, Part II: Source apportionment using positive matrix  
7 factorisation, *Environ. Chem.*, 8, 91–103, doi:10.1071/en10067, 2011
- 8 Goldstein, A. H. and Galbally, I. E.: Known and unexplored organic constituents in the  
9 earth's atmosphere, *Environ. Sci. Technol.*, 41, 1514–1521, 2007
- 10 Goldstein, A. H. and Schade, G. W.: Quantifying biogenic and anthropogenic contributions to  
11 acetone mixing ratios in a rural environment, *Atmos. Environ.*, 34, 4997–5006, 2000.
- 12 Guenther, A., Hewitt, C. N., Erickson, D., Fall, R., Geron, C., Graedel, T., Harley, P.,  
13 Klinger, L., Lerdau, M., McKay, W. A., Pierce, T., Scholes, B., Steinbrecher, R., Tallamraju,  
14 R., Taylor, J., and Zimmerman, P.: A global model of natural volatile organic compound  
15 emissions, *J. Geophys. Res.*, 100, 8873–8892, 1995
- 16 Guenther, A., Geron, C., Pierce, T., Lamb, B., Harley, P., and Fall, R.: Natural emissions of  
17 non-methane volatile organic compounds, carbon monoxide, and oxides of nitrogen from  
18 North America, *Atmos. Environ.*, 34, 2205–2230, 2000.
- 19 Heald, C. L., Jacob, D. J., Turquety, S., Hudman, R. C., Weber, R. J., Sullivan, A. P., Peltier,  
20 R. E., Atlas, E. L., de Gouw, J. A., Warneke, C., Holloway, J. S., Neuman, J. A., Flocke, F.  
21 M., and Seinfeld, J. H.: Concentrations and sources of organic carbon aerosols in the free  
22 troposphere over North America, *J. Geophys. Res.*, 111, D23S47, doi:  
23 10.1029/2006JD007705, 2006.
- 24 Hennigan, C. J., M. H. Bergin, J. E. Dibb, , and R. J. Weber, Enhanced secondary organic  
25 aerosol formation due to water uptake by fine particles, *Geophys. Res. Lett.*, 35, L18801,  
26 doi:10.1029/2008GL035046, 2008a
- 27 Hennigan, C. J., Bergin, M. H., and Weber, R. J.: Correlations between water-soluble organic  
28 aerosol and water vapor: a synergistic effect from biogenic emissions?, *Environ. Sci Technol.*,  
29 42, 9079–9085, 2008b
- 30 Hildebrandt, L., Engelhart, G. J., Mohr, C., Kostenidou, E., Lanz, V. A., Bougiatioti, A.,  
31 DeCarlo, P. F., Prevot, A. S. H., Baltensperger, U., Mihalopoulos, N., Donahue, N. M., and  
32 Pandis, S. N.: Aged organic aerosol in the Eastern Mediterranean: the Finokalia Aerosol  
33 Measurement Experiment – 2008, *Atmos. Chem. Phys.*, 10, 4167–4186, doi:10.5194/acp-10-  
34 4167-2010, 2010.
- 35 Holzinger, R., Warneke, C., Hansel, A., Jordan, A., Lindinger, W., Scharffe, D.H., Schade,  
36 G., and Crutzen, P. J.: Biomass burning as a source of formaldehyde, acetaldehyde, methanol,  
37 acetone, acetonitrile, and hydrogen cyanide, *Geophys. Res. Lett.*, 26, 1161–1164,  
38 doi:10.1029/1999GL900156, 1999.
- 39 Holzinger, R., Lee, A., Paw, K. T., and Goldstein, U. A. H.: Observations of oxidation  
40 products above a forest imply biogenic emissions of very reactive compounds, *Atmos. Chem.*  
41 *Phys.*, 5, 67–75, doi:10.5194/acp-5-67-2005, 2005.



- 1 Hopke, P. K.: A Guide to Positive Matrix Factorization, EPA Workshop Proceedings,  
2 Materials from the Workshop on UNMIX and PMF as Applied to PM<sub>2.5</sub>, 14–16 February,  
3 2000.
- 4 Hopke, P. K.: Recent developments in receptor modeling, *J. Chemometr.*, 17, 255–265,  
5 doi:10.1002/cem.796, 2003
- 6 Hu, L., Millet, D. B., Mohr, M. J., Wells, K. C., Griffis, T. J., and Helmig, D.: Sources and  
7 seasonality of atmospheric methanol based on tall tower measurements in the US Upper  
8 Midwest, *Atmos. Chem. Phys.*, 11, 11145–11156, doi:10.5194/acp-11-11145-2011, 2011.
- 9 Hu, L., Millet, D. B., Kim, S. Y., Wells, K. C., Griffis, T. J., Fischer, E. V., Helmig, D.,  
10 Hueber, J., and Curtis, A. J.: North American acetone sources determined from tall tower  
11 measurements and inverse modeling, *Atmos. Chem. Phys.*, 13, 3379–3392, doi:10.5194/acp-  
12 13-3379-2013, 2013.
- 13 Huang, X. F., and Yu, J. Z., Is vehicle exhaust a significant primary source of oxalic acid in  
14 ambient aerosols?, *Geophys. res. Lett.*, 34(2), 2007
- 15 Hwang, I. and Hopke, P. K.: Estimation of source apportionment and potential source  
16 locations of PM<sub>2.5</sub> at a west coastal IMPROVE site, *Atmos. Environ.*, 41, 506–518, 2007.
- 17 Jimenez, J. L., M. R. Canagaratna, N. M. Donahue, A. S. H. Prevot, Q. Zhang, J. H. Kroll, P.  
18 F. DeCarlo, J. D. Allan, H. Coe, N. L. Ng, A. C. Aiken, K. S. Docherty, I. M. Ulbrich, A. P.  
19 Grieshop, A. L. Robinson, J. Duplissy, J. D. Smith, K. R. Wilson, V. A. Lanz, C. Hueglin, Y.  
20 L. Sun, J. Tian, A. Laaksonen, T. Raatikainen, J. Rautiainen, P. Vaattovaara, M. Ehn, M.  
21 Kulmala, J. M. Tomlinson, D. R. Collins, M. J. Cubison, E., J. Dunlea, J. A. Huffman, T. B.  
22 Onasch, M. R. Alfarra, P. I. Williams, K. Bower, Y. Kondo, J. Schneider, F. Drewnick, S.  
23 Borrmann, S. Weimer, K. Demerjian, D. Salcedo, L. Cottrell, R. Griffin, A. Takami, T.  
24 Miyoshi, S. Hatakeyama, A. Shimono, J. Y Sun, Y. M. Zhang, K. Dzepina, J. R. Kimmel, D.  
25 Sueper, J. T. Jayne, S. C. Herndon, A. M. Trimborn, L. R. Williams, E. C. Wood, A. M.  
26 Middlebrook, C. E. Kolb, U. Baltensperger, and D. R. Worsnop, Evolution of Organic  
27 Aerosols in the Atmosphere, *Science*, 326, 1525-1529, 2009
- 28 Jobson, B. T., Wu, Z., Niki, H., and Barrie, L. A.: Seasonal trends of isoprene, C<sub>2</sub>-C<sub>5</sub> alkanes,  
29 and acetylene at a remote boreal site in Canada, *J. Geophys. Res.*, 99, 1589–1599, 1994
- 30 Kanakidou, M.A., Seinfeld, J.H., Pandis, S.N., Barnes, I., Dentener, F., Facchini, M.C., Van  
31 Dingenen, R., Ervens, B., Nenes, A., Nielsen, C.J., Swietlicki, E., Putaud, J.P., Balkanski, Y.,  
32 Fuzzi, S., Horth, J., Moortgat, G., Winterhalter, R., Myhre, C.E., Tsigaridis, K., Vignati, E.,  
33 Stephanou, E.G., Wilson, J., Organic aerosol and global climate modelling: a review, *Atmos.*  
34 *Chem. and Phys.*, 5, 1053-1223, 2005
- 35 Kawamura, K., Kasukabe, H., and Barrie, L. A., Source and reaction pathways of  
36 dicarboxylic acids, ketoacids and dicarbonyls in arctic aerosols: One year of observations,  
37 *Atmos. Environ.*, 30(10), 1709-1722, 1996
- 38 Kondo, Y., Miyazaki, Y., Takegawa, N., Miyakawa, T., Weber, R. J., Jimenez, J. L., Zhang,  
39 Q., and Worsnop, D. R.: Oxygenated and water-soluble organic aerosols in Tokyo, *J.*  
40 *Geophys. Res.*, 112, D01203, doi: 10.1029/2006jd007056, 2007.



- 1 Kroll, J. H. and Seinfeld, J. H.: Chemistry of secondary organic aerosol: Formation and  
2 evolution of low-volatility organics in the atmosphere, *Atmos. Environ.*, 42, 3593-3624, 2008
- 3 Lanz, V. A., Henne, S., Staehelin, J., Hueglin, C., Vollmer, M. K., Steinbacher, M.,  
4 Buchmann, B., and Reimann, S.: Statistical analysis of anthropogenic non-methane VOC  
5 variability at a European background location (Jungfraujoch, Switzerland), *Atmos. Chem.*  
6 *Phys.*, 9, 3445–3459, doi:10.5194/acp-9-3445-2009, 2009
- 7 Latella, A., Stani, G., Cobelli, L., Duane, M., Junninen, H., Astorga, C., and Larsen, B. R.:  
8 Semicontinuous GC analysis and receptor modelling for source apportionment of ozone  
9 precursor hydrocarbons in Bresso, Milan, 2003, *J. Chrom. A*, 39, 29–39, 2005
- 10 Lee, A., Goldstein, A. H., Keywood, M. D., Gao, S., Varutbangkul, V., Bahreini, R., Ng, N.  
11 L., Flagan, R. C., and Seinfeld, J. H.: Gas-phase products and secondary aerosol yields from  
12 the ozonolysis of ten different terpenes, *J. Geophys. Res.-Atmos.*, 111, D07302,  
13 doi:10.1029/2005jd006437, 2006.
- 14 Lelieveld J., Berresheim H., Borrmann S., Crutzen P.J., Dentener F.J., Fischer J., Flatau P.J.,  
15 Heland J., Holzinger R., Kormann R., Lawrence M.G., Levi Z., Markowicz K.M.,  
16 Mihalopoulos N., Minikin A., Ramanathan V., De Reus M., Roelofs G.J., Scheeren H.A.,  
17 Sciare J., Schlager H., Schultz M., Seigmund, P., Steil B., Stephanou E.G., Steir P., Traub M.,  
18 Warneke C., Williams J., Ziereis H., Global air pollution crossroads over the Mediterranean,  
19 *Science*, 298, 794-799, 2002
- 20 Leuchner, M. and Rappenglück, B.: VOC source–receptor relationships in Houston during  
21 TexAQS-II, *Atmos. Environ.*, 44, 4056– 4067, doi:10.1016/j.atmosenv.2009.02.029, 2010
- 22 Leuchner, M., Gubo, S., Schunk, C., Wastl, C., Kirchner, M., Menzel, A., and Plass-  
23 Dülmer, C.: Can positive matrix factorization help to understand patterns of organic trace  
24 gases at the continental Global Atmosphere Watch site Hohenpeissenberg?, *Atmos. Chem.*  
25 *Phys.*, 15, 1221-1236, doi:10.5194/acp-15-1221-2015, 2015.
- 26 Lim, H. J., Carlton, A. G., and Turpin, B. J.: Isoprene forms secondary organic aerosol  
27 through cloud processing: Model simulations, *Environ. Sci. Technol.*, 39, 4441–4446, 2005.
- 28 Lohmann, U. and Feichter, J.: Global indirect aerosol effects: a review, *Atmos. Chem. Phys.*,  
29 5, 715–737, doi:10.5194/acp-5-715-2005, 2005
- 30 MacDonald, R.C. and Fall, R.: Detection of substantial emissions of methanol from plants to  
31 the atmosphere, *Atmos. Environ.*, 27, 1709–1713, doi:10.1016/0960-1686(93)90233-O, 1993
- 32 Madronich, S.: Chemical evolution of gaseous air pollutants downwind of tropical megacities:  
33 Mexico City case study, *Atmos. Environ.*, 40, 6012–6018,  
34 doi:10.1016/j.atmosenv.2005.08.047, 2006
- 35 McKeen, S. A., Liu, S. C., Hsie, E.-Y., Lin, X., Bradshaw, J. D., Smyth, S., Gregory, G. L.,  
36 and Blake, D. R.: Hydrocarbon ratios during PEM-WEST A: a model perspective, *J.*  
37 *Geophys. Res.*, 101, 2087–2109, doi:10.1029/95JD02733, 1996.
- 38 Minguillón, M. C., Ripoll, A., Pérez, N., Prévôt, A. S. H., Canonaco, F., Querol, X., and  
39 Alastuey, A.: Chemical characterization of submicron regional background aerosols in the



- 1 western Mediterranean using an Aerosol Chemical Speciation Monitor, *Atmos. Chem. Phys.*,  
2 15, 6379–6391, doi: 10.5194/acp-15-6379-2015, 2015.
- 3 Minguillón, M. C., Pérez, N., Marchand, N., Bertrand, A., TemimeRoussel, B., Agrios, K.,  
4 Szidat, S., van Drooge, B. L., Sylvestre, A., Alastuey, A., Reche, C., Ripoll, A., Marco, E.,  
5 Grimalt, J. O., and Querol, X.: Secondary organic aerosol origin in an urban environment.  
6 Influence of biogenic and fuel combustion precursors, *Faraday Discuss.*, 189, 337–359, DOI:  
7 10.1039/c5fd00182j, 2016
- 8 Miyazaki, Y., Kondo, Y., Takegawa, N., Komazaki, Y., Fukuda, M., Kawamura, K.,  
9 Mochida, M., Okuzawa, K., and Weber, R. J.: Time-resolved measurements of water-soluble  
10 organic carbon in Tokyo, *J. Geophys. Res.*, 111, D23206, doi:10.1029/2006jd007125, 2006.
- 11 Miyoshi, A., Hatakeyama, S., and Washida, N.: OH radical-initiated photooxidation of  
12 isoprene: an estimate of global CO production, *J. Geophys. Res.-Atmos.*, 99, 18779–18787,  
13 1994.
- 14 Mohr, C., DeCarlo, P. F., Heringa, M. F., Chirico, R., Slowik, J. G., Richter, R., Reche, C.,  
15 Alastuey, A., Querol, X., Seco, R., Peñuelas, J., Jiménez, J. L., Crippa, M., Zimmermann, R.,  
16 Baltensperger, U., and Prévôt, A. S. H.: Identification and quantification of organic aerosol  
17 from cooking and other sources in Barcelona using aerosol mass spectrometer data, *Atmos.*  
18 *Chem. Phys.*, 12, 1649–1665, doi:10.5194/acp-12-1649-2012, 2012
- 19 Myriokefalitakis, S., Tsigaridis, K., Mihalopoulos, N., Sciare, J., Nenes, A., Kawamura, K.,  
20 Segers, A., and Kanakidou, M.: In-cloud oxalate formation in the global troposphere: a 3-D  
21 modeling study, *Atmos. Chem. Phys.*, 11, 5761–5782, doi:10.5194/acp-11-5761-2011, 2011.
- 22 Ng, N. L., Canagaratna, M. R., Zhang, Q., Jimenez, J. L., Tian, J., Ulbrich, I. M., Kroll, J. H.,  
23 Docherty, K. S., Chhabra, P. S., Bahreini, R., Murphy, S. M., Seinfeld, J. H., Hildebrandt, L.,  
24 Donahue, N. M., DeCarlo, P. F., Lanz, V. A., Prevôt, A. S. H., Dinar, E., Rudich, Y., and  
25 Worsnop, D. R.: Organic aerosol components observed in Northern Hemispheric datasets  
26 from Aerosol Mass Spectrometry, *Atmos. Chem. Phys.*, 10, 4625–4641, doi:10.5194/acp-10-  
27 4625-2010, 2010a
- 28 Ng, N. L., Canagaratna, M. R., Jimenez, J. L., Zhang, Q., Ulbrich, I. M., and Worsnop, D. R.,  
29 Real-time methods for estimating organic component mass concentrations from aerosol mass  
30 spectrometer data, *Environ. Sci. Tech.*, 45(3), 910–916, 2010b
- 31 Ng, N. L., Herndon, S. C., Trimborn, A., Canagaratna, M. R., Croteau, P. L., Onasch, T. B.,  
32 Sueper, D., Worsnop, D. R., Zhang, Q., Sun, Y. L., and Jayne, J. T.: An Aerosol Chemical  
33 Speciation Monitor (ACSM) for Routine Monitoring of the Composition and Mass  
34 Concentrations of Ambient Aerosol, *Aerosol Sci. Technol.*, 45, 780–794, doi:  
35 10.1080/02786826.2011.560211, 2011
- 36 Norris, G. A., Vedantham, R., Wade, K., Brown, S., Prouty, J., and Foley, C.: EPA Positive  
37 Matrix Factorization (PMF) 3.0: fundamentals & user guide, U.S. Environmental Protection  
38 Agency, 2008.
- 39 Orsini, D. A., Ma, Y., Sullivan, A., Sierau, B., Baumann, K., and Weber, R.: Refinements to  
40 the Particle-Into-Liquid Sampler (PILS) for ground and airborne measurements of water  
41 soluble aerosol composition, *Atmos. Environ.*, 37, 1243–1259, 2003.



- 1 Paatero, P. and Tapper, U.: Positive Matrix Factorization : anon-negative factor model with  
2 optimal utilization of error estimates of data values. *Environmetrics*, 5, 111-126, 1994
- 3 Paatero, P.: A weighted non-negative least squares algorithm for three-way 'PARAFAC' factor  
4 analysis. *Chemometrics and Intelligent Laboratory Systems*, 38, (2), 223-242, 1997
- 5 Paatero, P.: The multilinear engine – A table-driven, least squares program for solving  
6 multilinear problems, including the n-way parallel factor analysis model, *J. Comp. Graph.*  
7 *Stat.*, 8, 854–888, doi: 10.2307/1390831, 1999.
- 8 Park, J.-H., Goldstein, A. H., Timkovsky, J., Fares, S., Weber, R., Karlik, J., and Holzinger,  
9 R.: Eddy covariance emission and deposition flux measurements using proton transfer  
10 reaction – time of flight – mass spectrometry (PTR-TOF-MS): comparison with PTR-MS  
11 measured vertical gradients and fluxes, *Atmos. Chem. Phys.*, 13, 1439–1456,  
12 doi:10.5194/acp-13-1439-2013, 2013
- 13 Parrish, D. D., Hahn, C. J., Williams, E. J., Norton, R. B., Fehsenfeld, F. C., Singh, H. B.,  
14 Shetter, J. D., Gandrud, B. W., and Ridley, B. A.: Indications of photochemical histories of  
15 Pacific air masses from measurements of atmospheric trace species at Point Arena, California,  
16 *J. Geophys. Res.*, 97, 15883–15901, 1992.
- 17 Parrish, D. D., Stohl, A., Forster, C., Atlas, E. L., Blake, D. R., Goldan, P. D., Kuster, W. C.,  
18 and de Gouw, J. A.: Effects of mixing on evolution of hydrocarbon ratios in the troposphere,  
19 *J. Geophys. Res.-Atmos.*, 112, D10S34, doi:10.1029/2006JD007583, 2007.
- 20 Parworth, C., Fast, J., Mei, F., Shippert, T., Sivaraman, C., Tilp, A., Watson, T., and Zhang,  
21 Q.: Long-term measurements of submicrometer aerosol chemistry at the Southern Great  
22 Plains (SGP) using an Aerosol Chemical Speciation Monitor (ACSM), *Atmos. Environ.* 106,  
23 43–55, 2015.
- 24 Peltier, R. E., Weber, R. J., and Sullivan, A. P.: Investigating a Liquid-Based Method for  
25 Online Organic Carbon Detection in Atmospheric Particles, *Aerosol Sci. Technol.*, 41, 1117–  
26 1127, doi: 10.1080/02786820701777465, 2007.
- 27 Petit, J.-E., Favez, O., Sciare, J., Crenn, V., Sarda-Estève, R., Bonnaire, N., Mocnik, G.,  
28 Dupont, J.-C., Haeffelin, M., and Leoz-Garziandia, E.: Two years of near real-time chemical  
29 composition of submicron aerosols in the region of Paris using an Aerosol Chemical  
30 Speciation Monitor (ACSM) and a multi-wavelength Aethalometer, *Atmos. Chem. Phys.*, 15,  
31 2985–3005, doi: 10.5194/acp-15-2985-2015, 2015
- 32 Pope, C. A. and Dockery, D. W.: Health effects of fine particulate air pollution: Lines that  
33 connect, *J. Air Waste Manage. Assoc.*, 56, 709–742, 2006
- 34 Reissell, A., Harry, C., Aschmann, S. M., Atkinson, R., and Arey, J.: Formation of acetone  
35 from the OH radical- and O<sub>3</sub>-initiated reactions of a series of monoterpenes, *J. Geophys. Res.*,  
36 104, 13869– 13879, 1999
- 37 Ripoll, A., Minguillón, M. C., Pey, J., Jimenez, J. L., Day, D. A., Sosedova, Y., Canonaco, F.,  
38 Prévôt, A. S. H., Querol, X., and Alastuey, A.: Long-term real-time chemical characterization  
39 of submicron aerosols at Montsec (southern Pyrenees, 1570 m a.s.l.), *Atmos. Chem. Phys.*,  
40 15, 2935–2951, doi: 10.5194/acp-15-2935-2015, 2015.



- 1 Roukos, J., Plaisance, H., Leonardis, T., Bates, M., and Locoge, N.: Development and  
2 validation of an automated monitoring system for oxygenated volatile organic compounds and  
3 nitrile compounds in ambient air, *J. Chroma. A*, 1216, 8642–8651,  
4 doi:10.1016/j.chroma.2009.10.018, 2009.
- 5 Rudolph, J. and Johnen, F. J.: Measurements of light atmospheric hydrocarbons over the  
6 Atlantic in regions of low biological activity, *J. Geophys. Res.*, 95, 20583–20591,  
7 doi:10.1029/JD095iD12p20583, 1990
- 8 Sauvage, S., Plaisance, H., Locoge, N., Wroblewski, A., Coddeville, P., and Galloo, J. C.:  
9 Long term measurement and source apportionment of non-methane hydrocarbons in three  
10 French rural areas, *Atmos. Environ.*, 43, 2430–2441, doi:10.1016/j.atmosenv.2009.02.001,  
11 2009
- 12 Sciare, J., Cachier, H., Oikonomou, K., Ausset, P., Sarda-Estève, R., and Mihalopoulos, N.:  
13 Characterization of carbonaceous aerosols during the MINOS campaign in Crete, July–  
14 August 2001: a multi-analytical approach, *Atmos. Chem. Phys.*, 3, 1743–1757,  
15 doi:10.5194/acp-3-1743-2003, 2003.
- 16 Sciare, J., Oikonomou, K., Favez, O., Liakakou, E., Markaki, Z., Cachier, H., and  
17 Mihalopoulos, N.: Long-term measurements of carbonaceous aerosols in the Eastern  
18 Mediterranean: evidence of long-range transport of biomass burning, *Atmos. Chem. Phys.*, 8,  
19 5551–5563, doi:10.5194/acp-8-5551-2008, 2008.
- 20 Sciare, J., d'Argouges, O., Sarda-Estève, R., Gaimoz, C., Dolgorouky, C., Bonnaire, N.,  
21 Favez, O., Bonsang, B., and Gros, V.: Large contribution of water-insoluble secondary  
22 organic aerosols in the region of Paris (France) during wintertime, *J. Geophys. Res.-Atmos.*,  
23 116, D22203, doi: 10.1029/2011JD015756, 2011.
- 24 Seibert, P., Kromp-Kolb, H., Baltensperger, U., Jost, D. T., Schwikowski, M., Kasper, A. and  
25 Puxbaum, H.: Trajectory analysis of aerosol measurements at high alpine sites. EUROTRAC  
26 Symposium 94. Garmish-Partenkirchen, Germany, Academic Publishing BV The Hague,  
27 1994.
- 28 Seinfeld, J. H., Pandis, S. N.: *Atmos. Chem. and Phys.*, edited by: Wiley-Interscience, New  
29 York, 1998.
- 30 Simpson, I. J., Akagi, S. K., Barletta, B., Blake, N. J., Choi, Y., Diskin, G. S., Fried, A.,  
31 Fuelberg, H. E., Meinardi, S., Rowland, F. S., Vay, S. A., Weinheimer, A. J., Wennberg, P.  
32 O., Wiebring, P., Wisthaler, A., Yang, M., Yokelson, R. J., and Blake, D. R.: Boreal forest  
33 fire emissions in fresh Canadian smoke plumes: C1-C10 volatile organic compounds (VOCs),  
34 CO<sub>2</sub>, CO, NO<sub>2</sub>, NO, HCN and CH<sub>3</sub>CN, *Atmos. Chem. Phys.*, 11, 6445–6463,  
35 doi:10.5194/acp-11-6445-2011, 2011.
- 36 Slowik, J. G., Vlasenko, A., McGuire, M., Evans, G. J., and Abbatt, J. P. D.: Simultaneous  
37 factor analysis of organic particle and gas mass spectra: AMS and PTR-MS measurements at  
38 an urban site, *Atmos. Chem. Phys.*, 10, 1969–1988, doi:10.5194/acp-10-1969- 2010, 2010.
- 39 Sorooshian, A., Brechtel, F. J., Ma, Y. L., Weber, R. J., Corless, A., Flagan, R. C., and  
40 Seinfeld, J. H.: Modeling and characterization of a particle-into-liquid sampler (PILS),  
41 *Aerosol Sci. Tech.*, 40, 396–409, 2006



- 1 Sorooshian, A., Lu, M. L., Brechtel, F. J., Jonsson, H., Feingold, G., Flagan, R. C., and  
2 Seinfeld, J. H., On the source of organic acid aerosol layers above clouds, *Environ. Sci.*  
3 *Technol.*, 41(13), 4647-4654, 2007
- 4 Stein, A., Draxler, R., Rolph, G., Stunder, B., Cohen, M. and Ngan, F.: NOAA's HYSPLIT  
5 atmospheric transport and dispersion modeling system., *Bull. Amer. Meteor. Soc.*,  
6 doi:10.1175/BAMS-D-14-00110.1, 2015
- 7 Stohl, A.: Trajectory statistics-a new method to establish source-receptor relationships of air  
8 pollutants and its application to the transport of particulate sulfate in Europe, *Atmos.*  
9 *Environ.*, 30, 579-587, 1996.
- 10 Sullivan, A. P., Weber, R. J., Clements, A. L., Turner, J. R., Bae, M. S., and Schauer, J. J.: A  
11 method for on-line measurement of water-soluble organic carbon in ambient aerosol particles:  
12 Results from an urban site, *Geophys. Res. Lett.*, 31, L13105, doi:10.1029/2004GL019681,  
13 2004
- 14 Sullivan, A. P., Peltier, R. E., Brock, C. A., de Gouw, J. A., Holloway, J. S., Warneke, C.,  
15 Wollny, A. G., and Weber, R. J.: Airborne measurements of carbonaceous aerosol soluble in  
16 water over northeastern United States: Method development and an investigation into water-  
17 soluble organic carbon sources, *J. Geo-phys. Res.-Atmos.*, 111, D23S46, doi:  
18 10.1029/2006JD007072, 2006.
- 19 Thunis, P., Triacchini, G., White, L., Maffei, G., Volta, V.: Air pollution and emission  
20 reductions over the Po-valley: Air Quality Modelling and Integrated Assessment, 18th world  
21 IMACS Congress and MODSIM09 International Congress on Modeling and Simulation,  
22 Interfacing Modeling and Simulation with Mathematical and Computational Sciences, pp.  
23 2335-234, 2009
- 24 Tian, Y. Z., Shi, G. L., Han, S. Q., Zhang, Y. F., Feng, Y. C., Liu, G. R., Gao, L. J., Wu, J. H.,  
25 and Zhu, T.: Vertical characteristics of levels and potential sources of water-soluble ions in  
26 PM10 in a Chinese megacity, *Sci. Total Environ.*, 447, 1-9, 2013
- 27 Tyndall, G. S., Cox, R. A., Granier, C., Lesclaux, R., Moortgat, G. K., Pilling, M. J.,  
28 Ravishankara, A. R., and Wallington, T. J.: Atmospheric chemistry of small organic peroxy  
29 radicals, *J. Geophys. Res.*, 106, 12157-12182, 2001.
- 30 Ulbrich, I. M., Canagaratna, M. R., Zhang, Q., Worsnop, D. R., and Jimenez, J. L.:  
31 Interpretation of organic components from Positive Matrix Factorization of aerosol mass  
32 spectrometric data, *Atmos. Chem. Phys.*, 9, 2891-2918, doi:10.5194/acp-9-2891-2009, 2009.
- 33 Vlasenko, A., Slowik, J. G., Bottenheim, J. W., Brickell, P. C., Chang, R. Y. W., Maedonald,  
34 A. M., Shantz, N. C., Sjostedt, S. J., Wiebe, H. A., Leitch, W. R., and Abbatt, J. P. D.:  
35 Measurements of VOCs by proton transfer reaction mass spectrometry at a rural Ontario site:  
36 Sources and correlation to aerosol composition, *J. Geophys. Res.*, 114, D21305,  
37 doi:10.1029/2009JD012025, 2009
- 38 Volkamer, R., San Martini, F., Molina, L. T., Salcedo, D., Jimenez, J. L., and Molina, M. J.,  
39 A missing sink for gas-phase glyoxal in Mexico City: Formation of secondary organic  
40 aerosol, *Geophys. Res. Lett.*, 34(19), 2007



- 1 Warneck, P., In-cloud chemistry opens pathway to the formation of oxalic acid in the marine  
2 atmosphere, *Atmos. Environ.*, 37(17), 2423-2427, 2003
- 3 Weber, R. J., Sullivan, A. P., Peltier, R. E., Russell, A., Yan, B., Zheng, M., de Gouw, J.,  
4 Warneke, C., Brock, C., Holloway, J. S., Atlas, E. L., and Edgerton, E.: A study of secondary  
5 organic aerosol formation in the anthropogenic-influenced southeastern United States, *J.*  
6 *Geophys. Res.*, 112, D13302, doi: 10.1029/2007jd008408, 2007.
- 7 Wisthaler, A., Jensen, N. R., Winterhalter, R., Lindinger, W., and Hjorth, J.: Measurements of  
8 acetone and other gas phase product yields from the oh-initiated oxidation of terpenes by  
9 protontransfer-reaction mass spectrometry (ptr-ms), *Atmos. Environ.*, 35, 6181–6191, 2001.
- 10 Yuan, B., Shao, M., de Gouw, J., Parrish, D. D., Lu, S., Wang, M., Zeng, L., Zhang, Q., Song,  
11 Y., Zhang, J., and Hu, M.: Volatile organic compounds (VOCs) in urban air: how chemistry  
12 affects the interpretation of positive matrix factorization (PMF) analysis, *J. Geophys. Res.*,  
13 117, D24302, 1–17, doi:10.1029/2012JD018236, 2012.
- 14 Zannoni, N., Dusanter, S., Gros, V., Sarda Esteve, R., Michoud, V., Sinha, V., Locoge, N.,  
15 and Bonsang, B.: Intercomparison of two comparative reactivity method instruments in the  
16 Mediterranean basin during summer 2013, *Atmos. Meas. Tech.*, 8, 3851-3865,  
17 doi:10.5194/amt-8-3851-2015, 2015.
- 18 Zannoni, N., Gros, V., Sarda Esteve, R., Kalogridis, C., Michoud, V., Dusanter, S., Sauvage,  
19 S., Locoge, N., Colomb, A., and Bonsang, B.: Summertime OH reactivity from a receptor  
20 coastal site in the Mediterranean basin, *Atmos. Chem. Phys. Discuss.*, doi:10.5194/acp-2016-  
21 684, in review, 2016.
- 22 Zhang, Q., Jimenez, J., Canagaratna, M., Ulbrich, I., Ng, N., Worsnop, D., and Sun, Y.:  
23 Understanding atmospheric organic aerosols via factor analysis of aerosol mass spectrometry:  
24 a review, *Anal. Bioanal. Chem.*, 401, 3045–3067, 2011.



- 1 Table 1: Summary of VOC measurements performed at Cape Corsica during the ChArMEx
- 2 SOP2 field campaign. DL stems for Detection Limit

| Instrument                  | Time resolution | # species                      | # species > DL | Overall uncertainties (%) | DL range (ppt) | Examples         | Mean $\pm 1\sigma$ (ppt) | DL (ppt) |
|-----------------------------|-----------------|--------------------------------|----------------|---------------------------|----------------|------------------|--------------------------|----------|
| PTR-ToFMS                   | 10 min          | 16                             | 16             | 6-23                      | 7-500          | isoprene         | 194 $\pm$ 224            | 20       |
|                             |                 |                                |                |                           |                | sum terpenes     | 407 $\pm$ 462            | 15       |
|                             |                 |                                |                |                           |                | acetaldehyde     | 329 $\pm$ 118            | 50       |
|                             |                 |                                |                |                           |                | acetic acid      | 1152 $\pm$ 405           | 110      |
| online<br>GC/FID-FID        | 90 min          | 43 NMHC                        | 22             | 5-23                      | 10-100         | ethane           | 891 $\pm$ 187            | 50       |
|                             |                 |                                |                |                           |                | butane           | 65 $\pm$ 92              | 20       |
|                             |                 |                                |                |                           |                | propene          | 31 $\pm$ 13              | 10       |
|                             |                 | C2-C12                         |                |                           |                | ethyne           | 92 $\pm$ 49              | 20       |
|                             |                 |                                |                |                           |                | benzene          | 27 $\pm$ 12              | 10       |
|                             |                 |                                |                |                           |                | toluene          | 77 $\pm$ 65              | 20       |
| Online<br>GC/FID-MS         | 90 min          | 16 OVOCs                       | 22             | 5-14                      | 5-100          | $\alpha$ -pinene | 108 $\pm$ 77             | 10       |
|                             |                 |                                |                |                           |                | B-Pinene         | 141 $\pm$ 124            | 10       |
|                             |                 |                                |                |                           |                | limonene         | 31 $\pm$ 35              | 10       |
|                             |                 | C3-C7<br>6 NMHCs               |                |                           |                | ethanol          | 184 $\pm$ 79             | 20       |
|                             |                 |                                |                |                           |                | hexanal          | 101 $\pm$ 50             | 20       |
|                             |                 |                                |                |                           |                | nonane           | 8 $\pm$ 46               | 5        |
| Offline<br>solid adsorbants | 180 min         | 35 NMHCs                       | 28             | ~25                       | ~5             | decane           | 3 $\pm$ 3                | 5        |
|                             |                 |                                |                |                           |                | styrene          | 6 $\pm$ 5                | 5        |
|                             |                 | C5-C16<br>5 C6-C12 n-aldehydes |                |                           |                | hexanal          | 17 $\pm$ 13              | 5        |
|                             |                 |                                |                |                           |                | formaldehyde     | 2483 $\pm$ 868           | 40       |
| Offline<br>DNPH             | 180 min         | 16<br>C1-C8                    | 14             | ~25                       | 6-40           | acetone          | 3430 $\pm$ 1126          | 20       |
|                             |                 |                                |                |                           |                | MEK              | 481 $\pm$ 385            | 20       |
|                             |                 |                                |                |                           |                | MACR             | 59 $\pm$ 35              | 15       |
|                             |                 |                                |                |                           |                | GLY              | 146 $\pm$ 81             | 15       |

3  
4



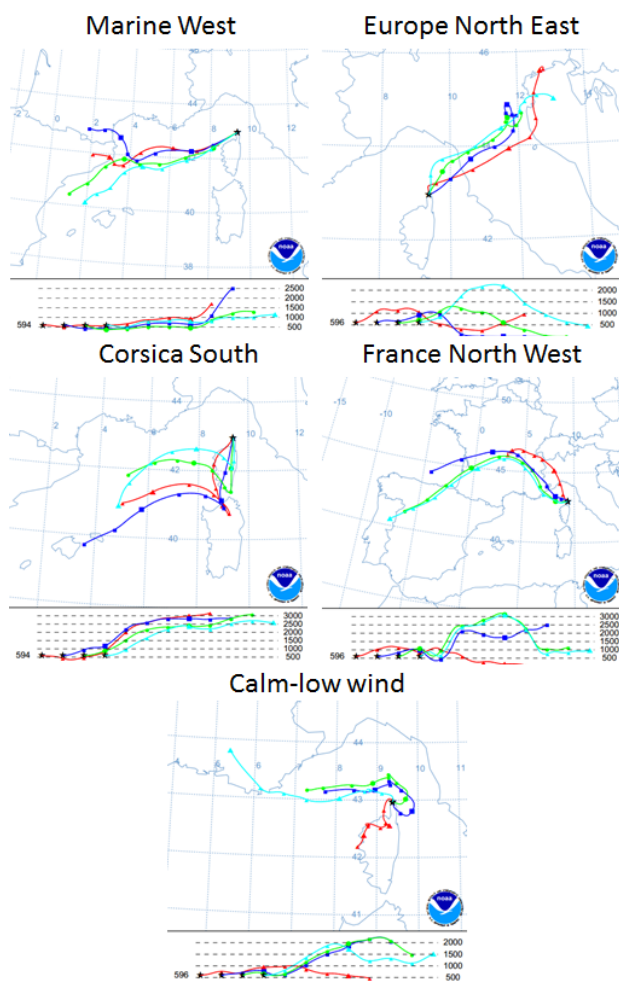
- 1 Table 2 : Back-trajectory clusters for the ChArMEx SOP2 field campaign in Cape Corsica.
- 2 The averaged transport time corresponds to the time spent since the last anthropogenic
- 3 contamination, i.e. since the air masses left the continental coasts.

| Clusters          | Source Region                  | Averaged transport Time | Contribution (%) |
|-------------------|--------------------------------|-------------------------|------------------|
| Marine West       | South France, North East Spain | 36 h->48 h              | 30%              |
| Europe-North East | North Italy                    | 10 h-20 h               | 26%              |
| Corsica South     | Corsica, Sardinia              | 12 h-24 h*              | 8%               |
| France-North West | South East france              | 12 h-18 h               | 6%               |
| Calm-Low wind     | Local                          | Not applicable          | 30%              |

- 4 \* For the Corsica-South cluster, the transport time corresponds to the time spent by the air
- 5 masses above land (Corsica and Sardinia Islands) before flying over the sea



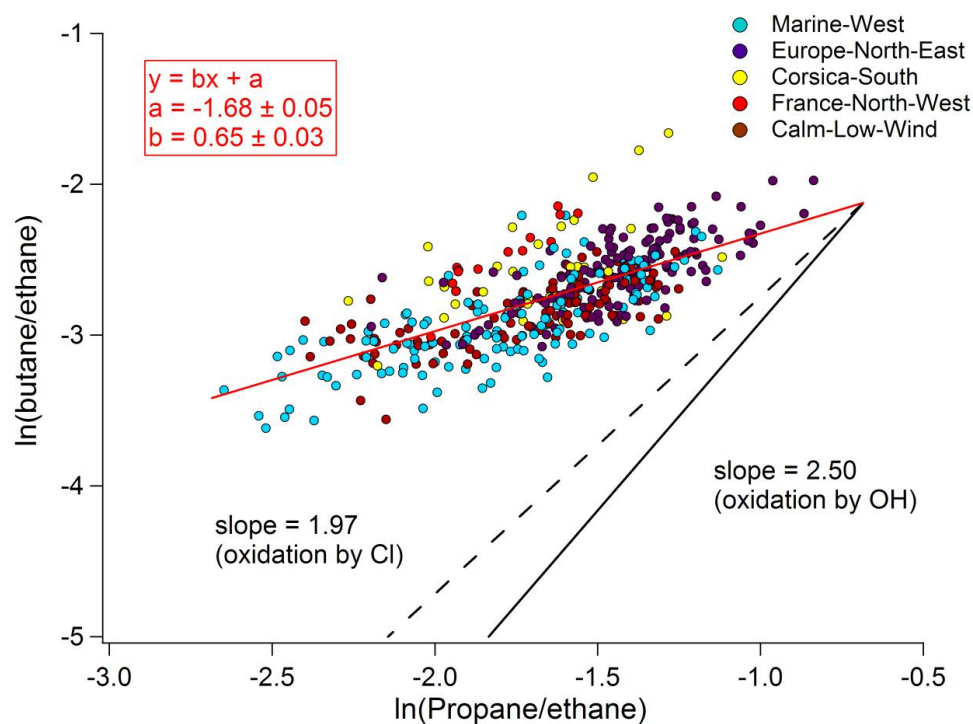
- 1
- 2 Figure 1: Localisation and geographical configuration of the measurement site at ERSA in
- 3 Cape Corsica (source: google map). The white solid square in the insert (top left) represents
- 4 the localisation of the city of Bastia.



1

2 Figure 2: Five Back-trajectory clusters identified for the ChArMEx SOP2 field campaign at  
3 Cape Corsica. This classification was conducted using back-trajectories calculated by the  
4 HYSPLIT Model (NOAA-ARL). The five clusters are illustrated by example maps for 4  
5 trajectories (interval of 6 hours between each, time of arrival indicates by different colours of  
6 trajectory) for five single days representatives of an isolated cluster (07/25, 07/21, 07/28,  
7 07/30 and 07/18 for Marine West, Europe-North East, Corsica South, France-West and Calm-  
8 low wind, respectively).

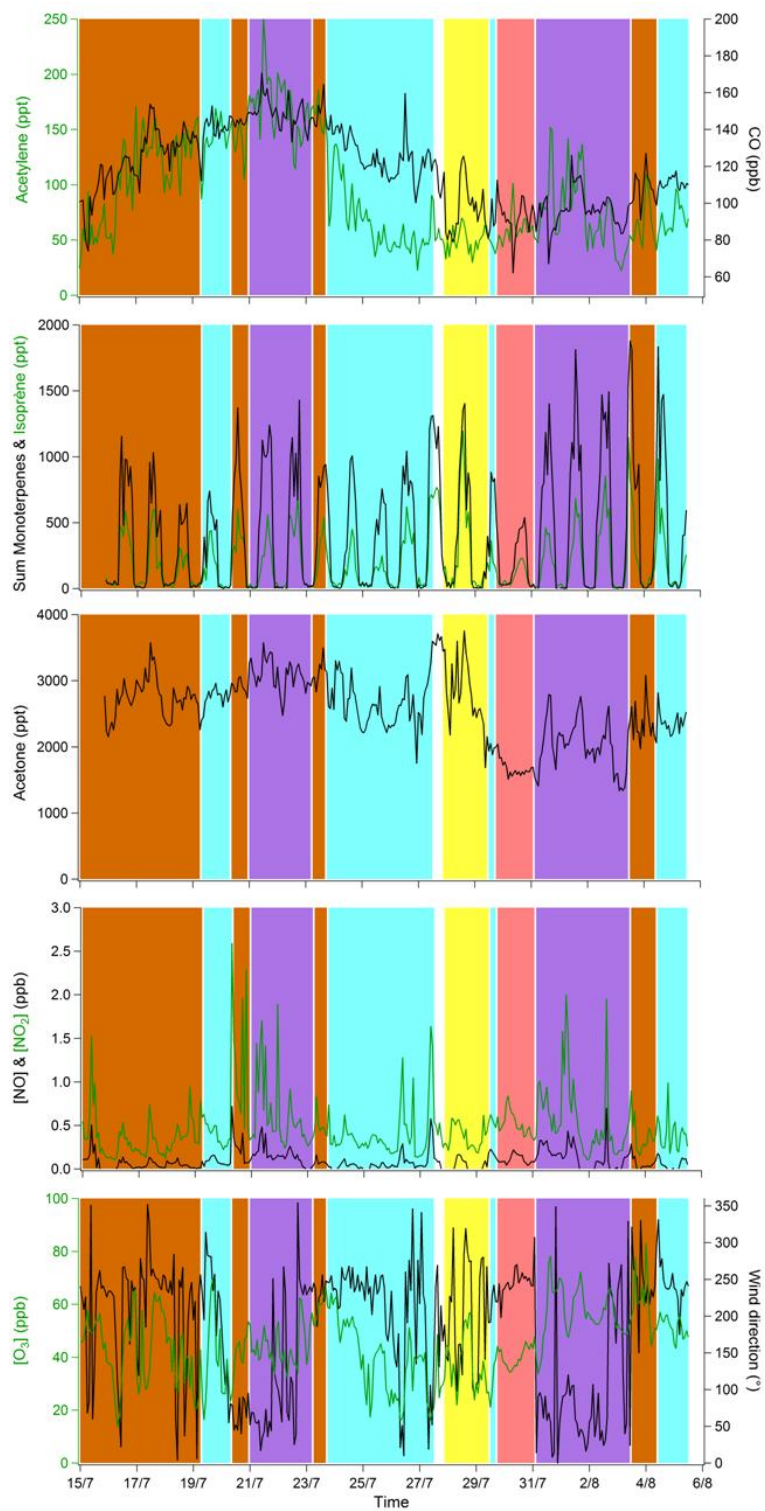
9



1

2 Figure 3 : Evolution of Ln(butane/ethane) as a function of Ln(propene/ethane) during the  
 3 ChArMEx SOP2 field campaign. The data were color-coded as a function of the back-  
 4 trajectory clusters (light blue, purple, yellow, red and brown for the Marine-West, Europe-  
 5 North-East, Corsica-South, France-North-West and Calm-Low-Wind clusters, respectively).  
 6 The red line corresponds to the linear regression. Black lines correspond to the theoretical  
 7 kinetic evolution of the ratios of alkanes due to oxidation by OH only (solid line) or Cl  
 8 only (dashed line).

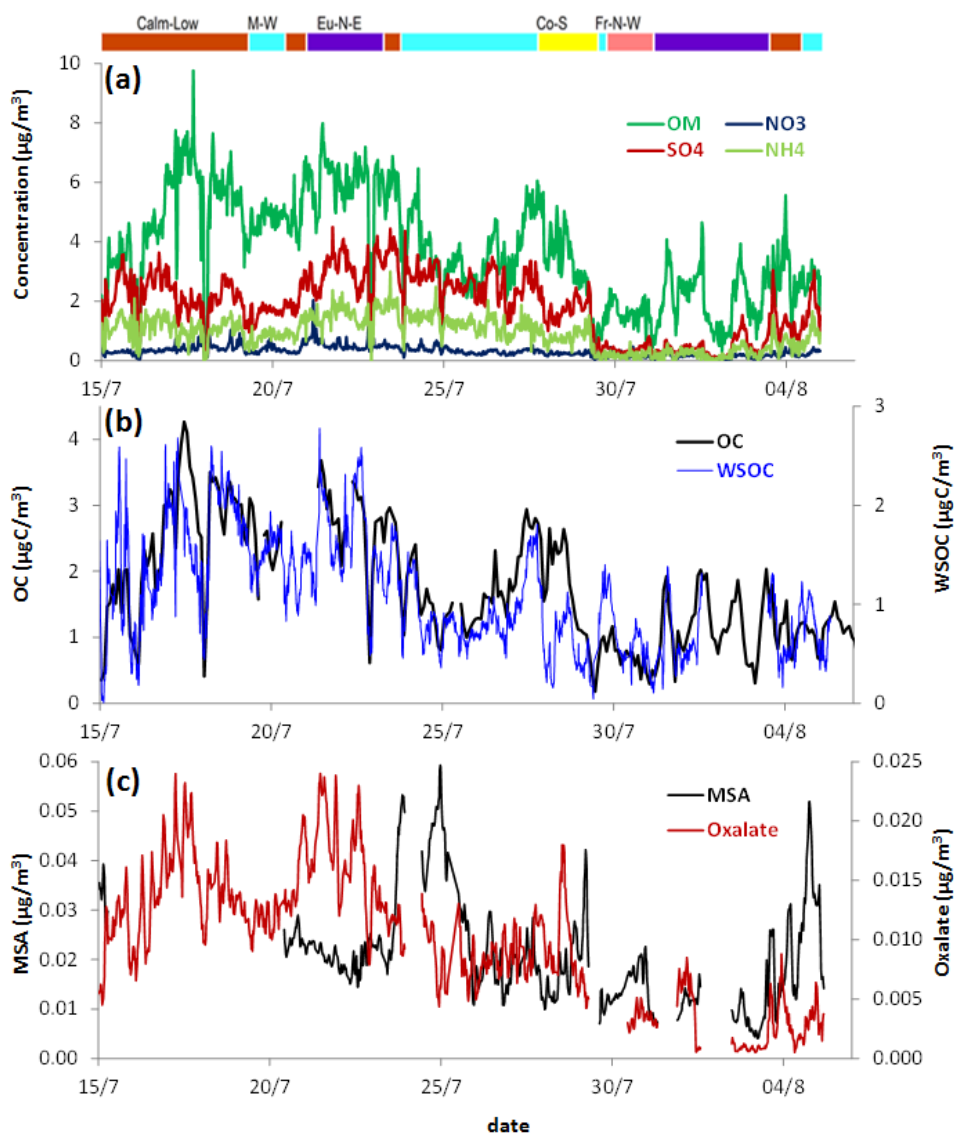
9





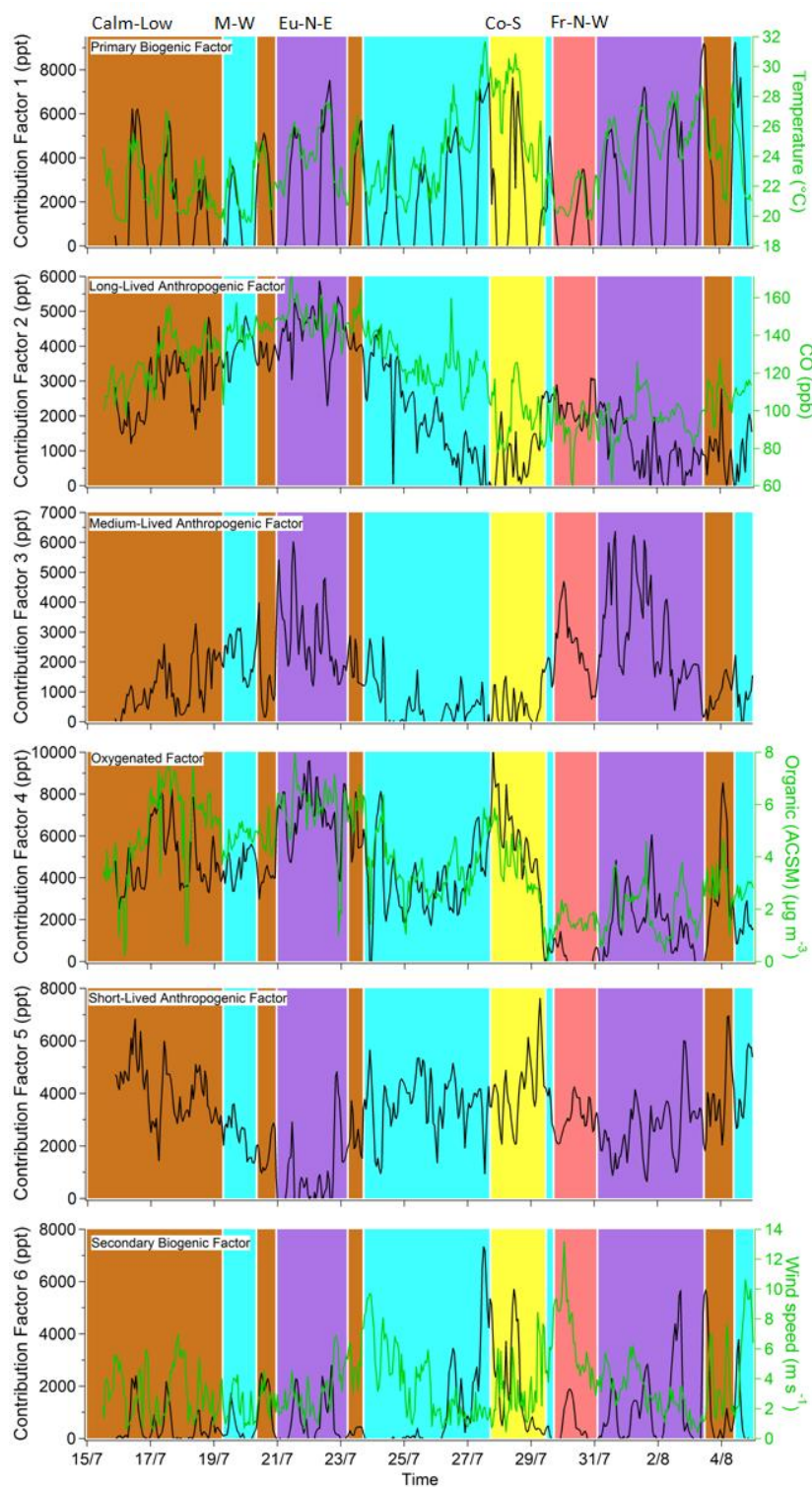
- 1 Figure 4: Time series of selected trace gases and wind direction at cape Corsica during the
- 2 ChArMEx SOP2 field campaign. The coloured areas correspond to back-trajectory clusters
- 3 (light blue, purple, yellow, pink and orange-brown for the Marine-West, Europe-North-East,
- 4 Corsica-South, France-North-West and Calm-Low-Wind clusters, respectively).

5



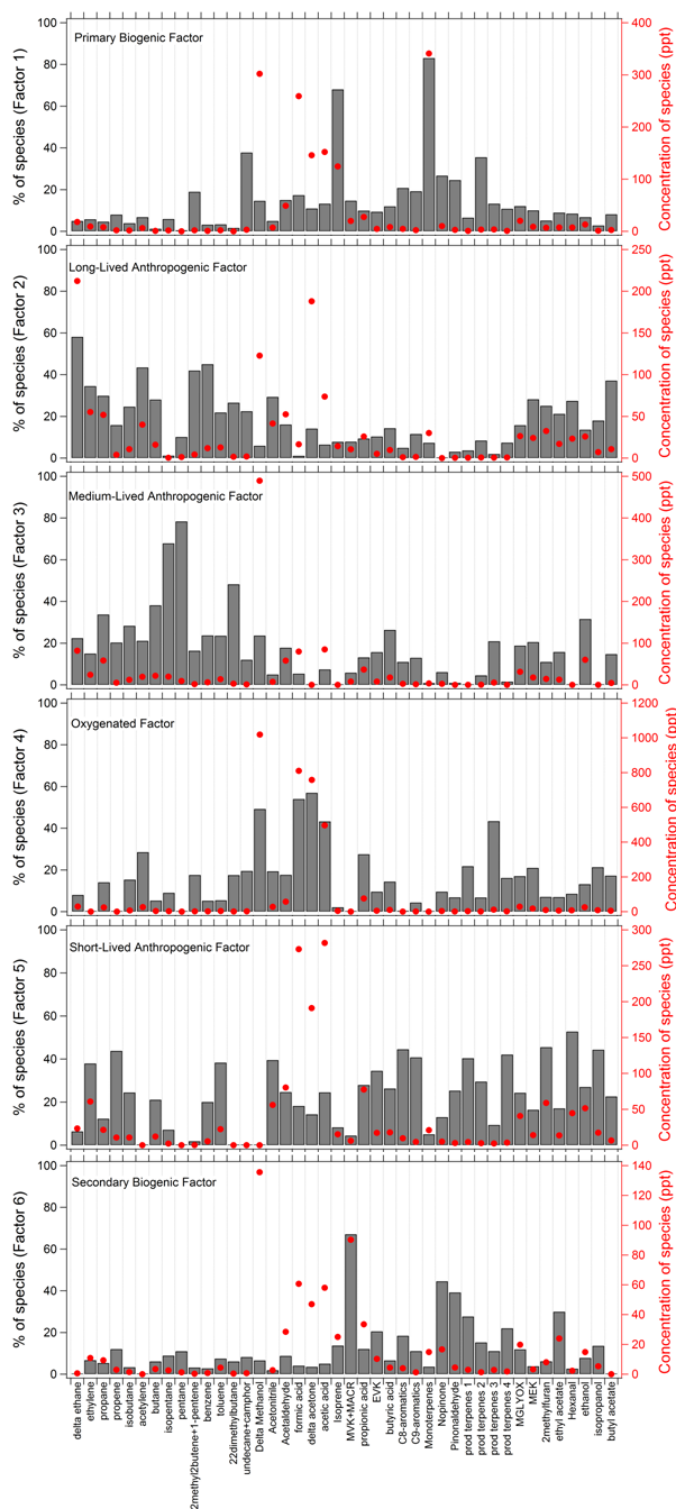
1

2 Figure 5: Temporal variability at Cape Corsica of (a) submicron (NR-PM<sub>1</sub>) chemical  
3 constituents measured by ACSM, (b) OC (PM<sub>2.5</sub>) and WSOC (PM<sub>1</sub>) measured by OCEC  
4 Sunset Field instrument and PILS-TOC, (c) MSA and oxalate (PM<sub>10</sub>) measured by PILS-IC.  
5 The coloured areas at the top correspond to back-trajectory clusters (light blue, purple,  
6 yellow, pink and orange-brown for the Marine-West (M-W), Europe-North-East (Eu-N-E),  
7 Corsica-South (Co-S), France-North-West (Fr-N-W) and Calm-Low-Wind (Calm-Low)  
8 clusters, respectively).





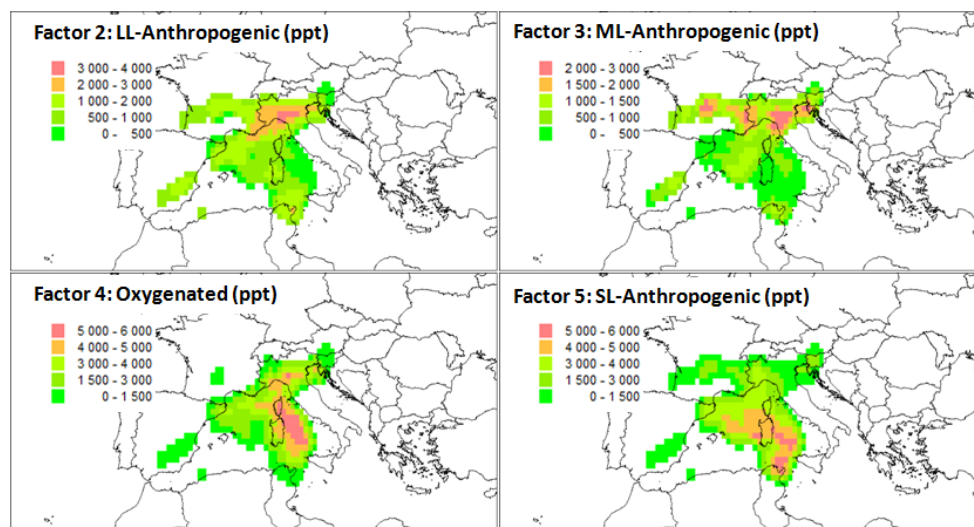
- 1 Figure 6: Time series for the contribution of the 6 gas-phase PMF factors together with
- 2 Temperature, CO, the measured Organic fraction of aerosols, and wind speed. The coloured
- 3 areas correspond to back-trajectory clusters (light blue, purple, yellow, pink and orange-
- 4 brown for the Marine-West (M-W), Europe-North-East (Eu-N-E), Corsica-South (Co-S),
- 5 France-North-West (Fr-N-W) and Calm-Low-Wind clusters, respectively).





1 Figure 7: Profiles of the 6 gas-phase PMF factors, with contributions of the factors to each  
2 species (black histograms, left axis in %) and contribution of the species to each factor (red  
3 circles, right axis in ppt). The “prod terpenes” 1, 2, 3 and 4 corresponds to the m/z 99, 111,  
4 113 and 155 signals from the PTR-ToFMS measurements, respectively, which have been  
5 attributed to oxidation products of terpenes (Holzinger et al., 2005; Lee et al., 2006; Vlasenko  
6 et al., 2009; Fares et al., 2012; Park et al., 2013).

7



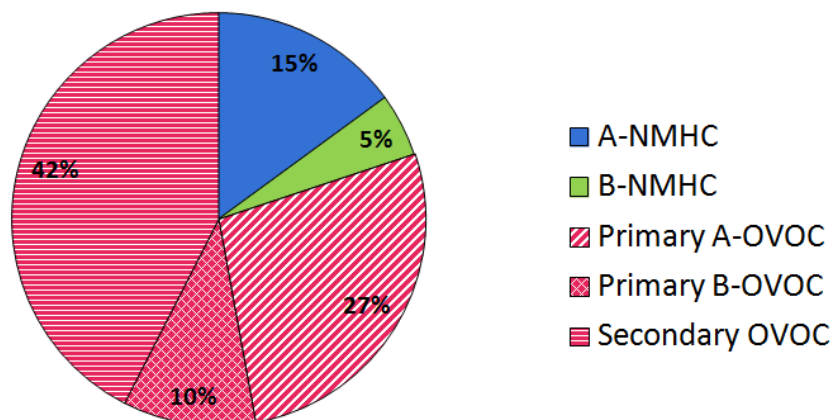
1

2 Figure 8: Source identification for the 6 gas-phase PMF factors, using the CF model.

3 Contributions are in units of ppt.

4

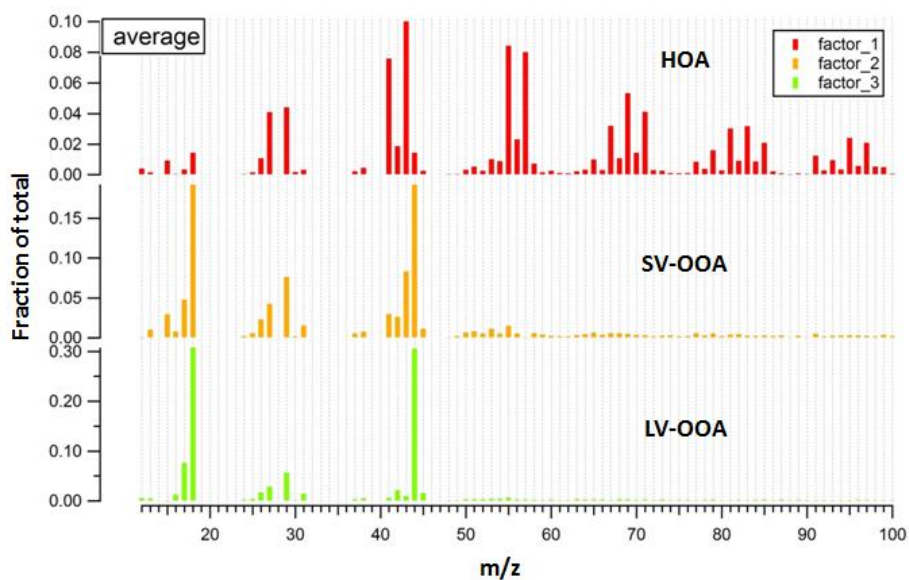
5



1

2 Figure 9: Distribution of the different VOC groups (ANMHC: Anthropogenic NMHCs (blue),  
3 BNMHC: Biogenic NMHCs (green), OVOC: Oxygenated VOCs (pink)), calculated from the  
4 database used for PMF analysis (same as bottom panel of Fig. S5). The OVOC group is  
5 divided into three sub-classes to account for their different origins: Primary anthropogenic  
6 (Primary A-OVOC, diagonal stripes), Primary biogenic (Primary B-OVOC, grid pattern) and  
7 secondary origin from the oxidation of both anthropogenic and biogenic VOCs (Secondary  
8 OVOC, horizontal stripes). The partitioning of these OVOCs into the three sub-classes is  
9 described in section 4.2.4.

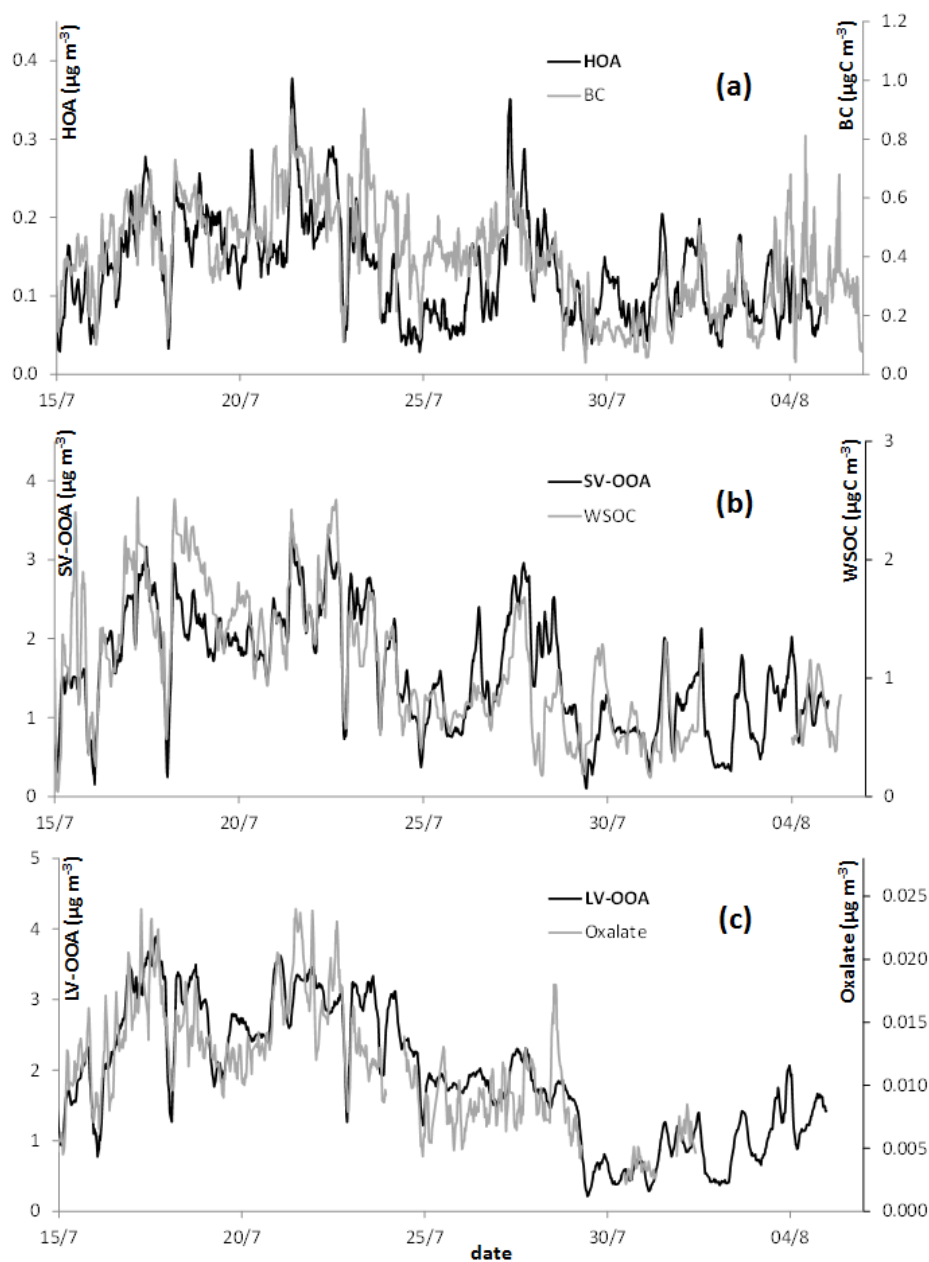
10



1

2 Figure 10 : Mass spectra profile obtained for the 3 factor constrained PMF solution (factor 1 =  
3 HOA (red); factor 2 = SV-OOA (orange); factor 3 = LV-OOA (green)).

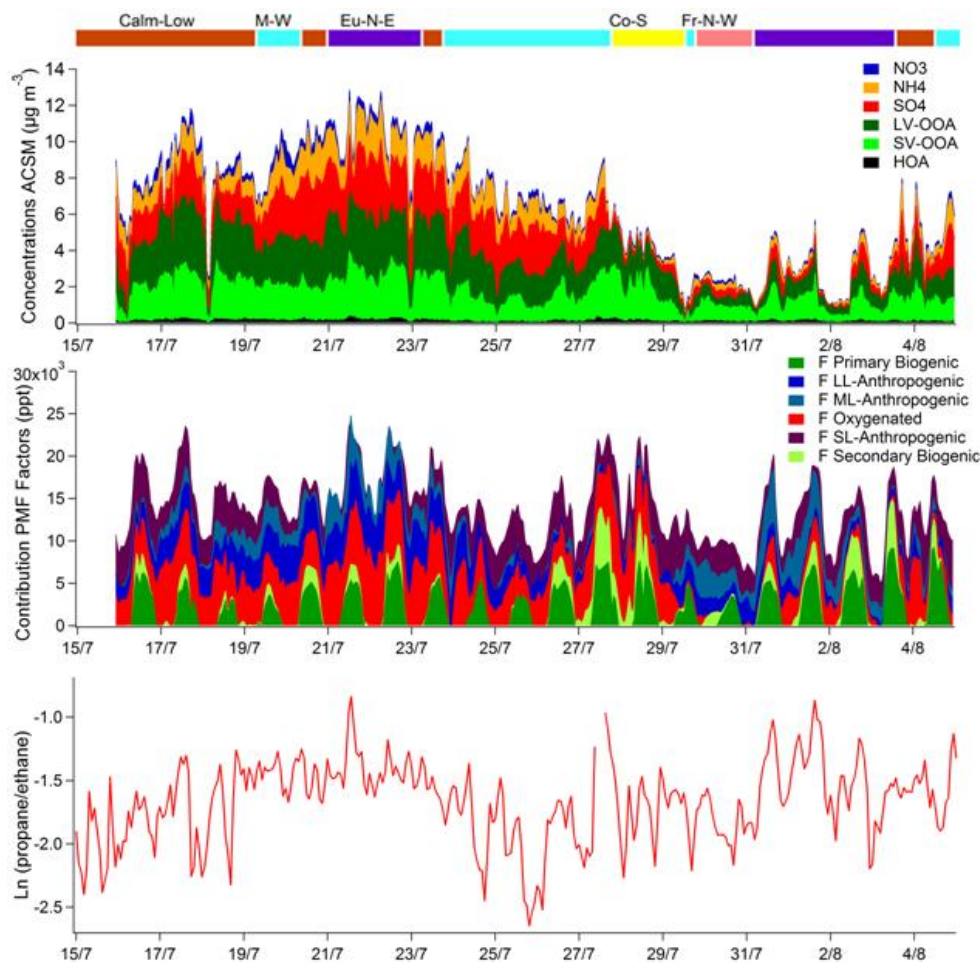
4



1

2 Figure 11 : Time-series of: (a) HOA (black) with Black Carbon (grey), (b) SV-OOA (black)  
3 with WSOC (grey), (c) LV-OOA (black) with oxalate (grey).

4



1

2 Figure 12 : Stacked time series of aerosol fractions (top panel), of VOC PMF Factors (middle  
3 panel), and of Ln(propene/ethane) as a proxy for photochemical age (bottom panel). F-LL, F-  
4 ML and F-SL-Anthropogenic refer to the Long-Lived, Medium-Lived and Short-Lived  
5 Anthropogenic factors, respectively. Coloured areas at the top correspond to back-trajectory  
6 clusters (light blue, purple, yellow, pink and orange-brown for the Marine-West (M-W),  
7 Europe-North-East (Eu-N-E), Corsica-South (Co-S), France-North-West (Fr-N-W) and Calm-  
8 Low-Wind (Calm-Low) clusters, respectively).

9